

Ministry of Higher Education
and Scientific Research
Babylon University
College of Engineering
Department of Civil Engineering



Flexural Behavior of Reinforced High Strength Concrete One Way Ribbed Slab Strengthened by Carbon Sheets

A Thesis Submitted to:

the College of Engineering at University of Babylon in Partial
Fulfillment of the Requirements for the Degree of Master in
Engineering /Civil Engineering /Structures

By:

Salwa Raid Jasim

Supervised by:

Dr. Hayder M. J. Al-Khafaji

بِسْمِ اللَّهِ الرَّحْمَنِ الرَّحِيمِ

{وَمَنْ يَتَوَكَّلْ عَلَى اللَّهِ فَهُوَ حَسْبُهُ إِنَّ اللَّهَ بَالِغُ أَمْرِهِ
قَدْ جَعَلَ اللَّهُ لِكُلِّ شَيْءٍ قَدْرًا }

صِرَاحُ اللَّهِ وَالْعَظِيمِ

[سورة الطلاق: الآية 3]

Dedication

To my family....

To my amazing mam...

To my friends ..

*To the one I missed a lot my darling
father, as you look down from heaven
I hope you proud of your little girl....*

Salwa Raid

Acknowledgement

In the name of Allah, the most gracious, the most merciful

All thanks and praise to Allah who enabled me to achieve this research work. Firstly, I would like to express my sincerest gratitude to my supervising Dr. Hayder M. J. Al-Khafaji, for his invaluable insight, wisdom, and guidance.

I would like to thank the support staff of the Department of Civil Engineering of Babylon University for their assistance with daily matters throughout my graduate academic life. Also, thanks to the technical staff of the structural laboratories for their assistance during the undertaking of my experimental program.

I would like to acknowledge the friendly support and assistance of my fellow graduate students who made my overall experience more gratifying.

Finally, a special thanks and gratitude to my family for their care, and patience. Without their love, encouragement, and support I would not have been able to complete this academic achievement.

List of contents

	1
Acknowledgement.....	IV
List of contents	V
1	V
List of Figures	VIII
Chapter One.....	1
1 Introduction.....	1
1.1 One Way Ribbed Slab.	1
1.2 Strengthening or Rehabilitation of Reinforcement Concrete.....	2
1.3 High Strength Concrete	3
1.4 Aims of The Project.....	4
1.5 Layout of Thesis	5
Chapter Two.....	7
2 Literature Review.....	7
2.1 Introduction.	7
2.2 Waffle slab or ribbed slab.....	7
2.3 Strengthening with CFRP.....	16
2.4 Summery.....	24
Chapter Three.....	27
3 Experimental Program	27
3.1 Introduction	27
3.2 Specimens Description	27
3.3 Specimens Preparation	30
3.3.1 Reinforcement Cages	31
3.3.2 Mold Preparation.....	31
3.3.3 Mix Design.....	32
3.3.4 Mixing Procedure, Casting and Curing.	33

3.3.5	Strengthening of The Specimens	35
3.4	Material Properties	36
3.4.2	Reinforcing Steel Bar	40
3.4.3	Epoxy	41
3.5	Harden Concretes Test	41
3.5.1	Compressive Strength	41
3.5.2	Tensile Strength	41
3.5.3	Modulus of Rupture	42
3.6	Test Instruments	43
3.6.1	Testing Machine	43
3.6.2	Supporting and load conditions	44
3.6.3	LVDT	45
3.7	Test procedure	46
Chapter Four	48
4	Experimental Results and Discussions	48
4.1	Introduction	48
4.2	Mechanical properties of concrete.....	48
4.3	Test result of the specimens.	49
4.3.1	Load- deflection curve and ultimate load	50
4.3.2	4.3.1 Group One.....	50
4.4	Stiffness	54
4.5	Modes of failure.....	56
4.5.1	Group one.....	56
4.5.2	Group two.....	56
4.5.3	Group three.....	59
4.6	Crack pattern.....	62
4.6.1	Group one.....	62

4.6.2	Group two.....	63
4.6.3	Group three.....	64
4.7	Ductility	65
4.7.1	Group two.....	66
4.7.2	Group three.....	66
4.7.3	Energy-Absorption.....	67
4.8	Theoretical Analysis and Comparison of Moment.	69
Chapter	72
5	Finite Element Analysis.....	72
5.1	General.....	72
5.2	Modeling of HSC One Way-Ribbed Slab strengthening with CFRP sheet.....	72
5.2.1	Types of elements.	72
5.2.2	Materials' properties.	73
5.2.3	Geometry and the Bond Condition.	77
5.3	Meshing and Converging Analysis.	79
5.4	Result and discussion.	79
5.4.1	Load – Deflection Curve Response.	79
5.5	Stress Behavior of CFRP at Ultimate load.....	82
5.6	Crack pattern.....	83
Chapter Six	88
6	Conclusions and Recommendations for Future Work.....	88
6.1	General.....	88
6.2	Conclusions from Experimental Works.	88
6.2.1	Types of Concrete.	88
6.2.2	Width of CFRP Sheets.	88
6.3	Conclusions from FE analysis.....	90
6.4	Recommendations for future study.	91

7	References	93
4	الخلاصة	1

List of Figures

Figure 1-1	one -way ribbed slab of [2] .	2
Figure 1-2	Rehabilitation of structure in Mosul.	3
Figure 7-1	show displacement measurement[12]	10
Figure 7-2	show the location of strain gauges and displacement control point [12].	11
Figure 7-3	Test setup for one- way ribbed slab[15]	15
Figure 7-4	Test setup for two- way ribbed slab[15]	15
Figure 7-5:	Details OF beam strengthening with CFRP sheet[20]	23
Figure 8-1	Definition of description specimens name.	28
Figure 8-2	The dimension and steel reinforcement of all tested ribbed	29
Figure 8-3	Ribs' bottom of group three specimens.	29
Figure 8-4	Steel reinforcement preparation.	31
Figure 8-5	Mold preparation for casting and steel reinforcement installation.	32
Figure 8-6	Mix preparing and casting.	34
Figure 8-7	Curing and preparing samples for strengthening.	34
Figure 8-8	Strengthening procedure from applying the adhesive and pointing the required CFRP places and installing the CFRP.	35
Figure 8-9	Test of SO ₃ content in sand.	37
Figure 8-10	Steel tensile test.	40
Figure 8-11	Compressive strength test, {a} the compressive strength device, {b} compressive failure of HSC, {c} compressive failure of NC.	41
Figure 8-12	Split tensile test, {a} testing device, {b} tensile failure of NC, {c} tensile failure of HSC.	42

Figure 3-8-13 Modules of rupture test, {a} testing device, {b} flexural failure in NC, {C} flexural failure in HSC.....	43
Figure 8-16 Position of LVDT.....	45
Figure 8-17 Test procedure from transporting the specimens to installation of all the tested specimens.....	46
Figure 4-1 Load-deflection curve of group one.....	50
Figure 4-2 Group two, specimens without additional strips.....	52
Figure 4-3 Load-mid span deflection for group two, specimens with additional U-shaped strips.....	53
Figure 4-4 Load-mid-span deflection curve for group two to specimens without U-shaped strips.....	54
Figure 4-5 Load- mid span deflection curve for group two to specimens with U-shaped strips.....	54
Figure 4-6 Comparative between stiffness for all groups.....	56
Figure 4-7 Type of failure on HCS-L1R50, steel yielding follow by CF sheet debonding.....	57
Figure 4-8 Rapture of CF sheet on HCS-L1R100	57
Figure 4-9 Flexural failure on HCS-L1R50.....	58
Figure 4-10 Flexural failure on HCSS-L1R100 by concrete cover separation.....	58
Figure 4-11 CF sheet raptured on HCS-L1WR	59
Figure 4-12 Flexural failure on HCS-L2R50.....	59
Figure 4-13 Flexural failure on HCS-L2R100 by CFRP fractured.	60
Figure 4-14 Flexural failure on HCSS-L2R50 by fractured of CF sheet	60
Figure 4-15 failure on HCSS-L2R100.....	61
Figure 4-16 Rapture of CF sheet on HCS-L2WR.....	61
Figure 4-17 Cracks pattern of group's one specimens.....	62
Figure 4-18 Cracks pattern for group two.....	64
Figure 4-19 Cracks pattern of group three.....	65

Figure 4-20 Show the method used to calculate the yielding deflection.	65
Figure 4-21 Compression between ductility of all samples.....	67
Figure 4-22 Energy absorption for group two.	68
Figure 4-23 Energy-Absorption for group three.	68
Figure 4-24 The neutral axis depth variation throuh the load stages.....	70
Figure 5-1 stress-strain in compression and in tension.....	75
Figure 5-2 Ribbed -slab concrete modeling.....	78
Figure 5-3 Steel reinforcement modeling.	78
Figure 5-4 Modeling of boundary condition and symmetry.....	78
Figure 5-5 Deflection at 37 kN in different mesh size.....	79
Figure 10-6 Load- deflection curve for group three.	81
Figure 5-7 Stress distributions in modeled specimens.....	83
Figure 5-8Crack in HCSS-R100	84
Figure 5-9 Cracks in HCS-R50.....	85
Figure 5-10 Cracks in WR.	86
Figure 5-11 Cracks pattern in HC.....	86

List of Tables

Table 2-1 show details of tested specimens	11
Table 2-2 show samples details [14].....	13
Table 2-3 details of tested beam[18].....	17
Table 2-4 the test result[3]	20
Table 3-1 Details of all tested groups' specimens.	30
Table 3-2 mix design percentage for both NC and HSC.	33
Table 3-3 The chemical analysis and main components in cement.	36
Table 3-4 The physical analysis of cement.....	37
Table 3-5 Sieve analysis of fine aggregate and comparison with Iraqi specification.	38
Table 3-6 Sieve analysis for coarse aggregate	39
Table 3-7 Typical properties from manufactured.....	39
Table 3-8 Typical properties for super plasticizer	40
Table 3-9 test result for steel reinforcing bars	40
Table 4-1 show the concrete mechanical properties.....	49
Table 4-3 show the first crack-load.....	63
Table 4-4comparing between specimens ductility.....	66
Table 4-5 Energy-absorption values for all groups.....	68
Table 4-6 The comparative of ultimate moment between experimental and theoretical analysis.	70
Table 5-1 The input data of concrete plasticity parameters.....	73
Table 5-2 The input data for all steel's bares and stirrups (isotropic / plastic).	75
Table 5-3 The input data on the equation which were used (value took from Reddy2004[11])).	77
Table 5-4 the experimental and F.E analysis	80

Abstract

In the last century, the strengthening of structures has taken place in all research around the world specially to strength or rehab the old structures that need to maintenance. A lot of areas were exposed to sever accident like war such as AL-Mosul that led to rehab many structures and since the concrete was harmful to the environment and the steel was not recommended to be used externally, because its ability of corrosion, the fiber reinforcement polymer be the suitable solution.

In this study, the structure is chosen to test the flexural behavior of strengthening with carbon fiber polymer sheet was the one –way Ribbed slab. All the specimens had same dimensions (200*600*2000) mm and the clear span was 1700mm. Twelve simply supported specimens were tested under one-line load to ensure the flexural failure and were divided in three groups. Group one had two specimens without strengthening one of them was cast with normal concrete C30, and the second was cast with high strength concrete C60. Second group included five high strength concrete specimens strengthened with different width of carbon sheet 50% and 100% from the rib's width, 50% and 100% with addition to U-shaped strips @250 mm and the last specimen wrapped all the ribs. All the specimens of group two had same strengthening length of 1240mm which was the minimum strengthening length required from ACI-code, while group three contained five specimens with the same Carbon's width as the second group, but with different length 1700mm (as the length of clear span).

It was found from the experimental work that strengthening with carbon's sheet raised the strength of structures and also make the structure stiffer. For group two, the ultimate load raised from 23% when using 50% carbon sheet from rib's width to 133% when the carbon sheet wrapped all the ribs. While group three raised the ultimate load from 3% when 50% carbon sheet was used and 167% when the carbon wrapped all the ribs. The length of carbon sheet had no effect on stiffness while it has effect on the ductility of the structures.

The second part of this investigation was the Finite Element analysis by using ABAQUS which was done on the samples of group three to compare the model that was used. The concrete was modeled by Concrete Damage

Plasticity and the carbon fiber sheet by orthotropic elastic materials. Numerical result compared with obtained result from experimental work in term of ultimate load –mid span deflection and the crack pattern. The result from ABAQUS program have good accuracy with the experimental result.

CHAPTER ONE

INTRODUCTION

Chapter One

1 Introduction

1.1 One Way Ribbed Slab.

A slab is a segment of reinforced concrete that forms a bigger structure and is often subjected to bending (tensile or compressive). It may, however, be sheared in extreme circumstances, such as a bridge deck. In some buildings, such as auditoriums, vestibules, theater halls, and show rooms, where column-free space is a need, it's important to design a slab that offers the best possible balance of safety, utility, and economics. In addition, these constructions require huge spans, and large spans require a lot of steel reinforcement, which led to thicker slabs and heavier structural members, which could cause the slab to collapse under its own weight. Instead of using solid slabs, new forms of slabs were developed to solve these issues. The optimal design was to remove concrete from portions of the slab that are not required for strength while thickening a part, so that reinforcement can be inserted at a deeper depth. As a result, numerous investigations and experiments have been conducted to find novel member types that could fulfill these needs. One of these members is a slab with one direction of ribs. A one-way ribbed floor slab is made up of numerous tiny reinforced concrete T beams joined by girders as shown in Figure1-1, which are itself supported by building columns. T beams, also referred to as joists, are created by positioning steel pan at regular intervals. While order to create the ribs, concrete is cast between the spaces; in doing so, the slab is also cast and becomes the flange of the T beam [1].



1-1 one -way ribbed slab of [2] .

1.2 Strengthening or Rehabilitation of Reinforcement Concrete.

The majority of reinforced concrete structures worldwide are degrading as a result of adverse environmental factors, rising service loads, and faults in design and construction. Existing RC structures need to be reinforced because of their age[3].The usage of fiber reinforced polymer (FRP) strips attached to the member's tensile face is one of the most promising solutions to these needs. In-depth experimental studies carried out in the past have demonstrated that this strengthening process offers a number of benefits more than the conventional , particularly because the composite material's improved durability, lightweight, and great strength[4]. The load-bearing strength and stiffness of the strengthened samples had been shown to be significantly improved by the technique of attaching CFRP plates or sheet to the tensile region of the beam utilizing epoxy adhesives. Numerous experimental and numerical studies on RC beams with strengthened flexure were conducted, and the conclusions indicated that when externally bonded to the tensile

surface of such beams, Comparing the strengthened specimens to the control (unstrengthened specimens), CFRP laminates enhanced the flexural capacity up to 100%[5]. FRP composites have been used to strengthen concrete buildings for more than decade; the most popular technique of reinforcing structures is through bending; however, column wrapping is also quite popular. Additionally, concrete columns, beams, slabs, and other shear-resistant constructions need to be strengthened[6]. Figure1-2 show Rehabilitation of some structures by CFRP sheet in Iraq.



Figure 1-2 Rehabilitation of structure in Mosul.

1.3 High Strength Concrete

Because the idea of high-strength concrete has changed over time, the Committee developed a spectrum of concrete strengths for its operations, as described in ACI 363R [7], high-strength concrete is defined as having a specified compressive strength of at least 55MPa. High-rise buildings, bridges, and offshore structures were the first applications for HSC, but it has since been extended to include, port and coastal buildings, hydraulic structures,

subterranean construction, factory floors, sidewalks, water treatment plants, and warehouses for hazardous waste as well as concrete products and chemicals, the durability attributes were crucial in certain applications, whilst the mechanical qualities were crucial in others. Nevertheless, the combined, enhanced, mechanical, and durable properties were typically the basis for the variety of uses, for different partners in new ventures, the value and advantages of employing HSC varied. Enhancements to features including improved compressive strength, modulus of elasticity, durability, speedy achievement of ultimate creep, and reduced dead load were given priority by the designer. The maker of concrete saw a growth in sales and market share thanks to high-tech manufacturing, which also benefited conventional production. Increased service life and cost-savings on cement and aggregate helped create a structure that was more ecologically friendly [8].

1.4 Aims of The Project

- 1- Comparison between flexural behavior of reinforcement one way ribbed slab by using normal concrete and high strength concrete.
- 2- Flexural strengthening of high strength concrete one-way ribbed slab by using externally bonded carbon fiber reinforced polymer sheet.
- 3- Three dimensional nonlinear finite element analysis has been used to conduct the numerical investigation of the general behavior of strength slab by using ABAQUS.

1.5 Layout of Thesis

- ❖ Chapter one shows an introduction about slab and strength reinforcement concrete.
- ❖ Chapter two includes a literature review of studies related to one way ribbed slab and/ or strength of reinforcement concrete and high strength concrete.
- ❖ Chapter three presents the experimental work, material properties and description of the mold and reinforcement of the specimens.
- ❖ Chapter four shows analysis and discussion of the experimental result.
- ❖ Chapter five includes ABAQUS analysis, details of the specimens and result of finite element method.
- ❖ Chapter six presents conclusions and recommendations for future studies.

CHAPTER TWO
LITERATURE REVIEW

Chapter Two

2 Literature Review

2.1 Introduction.

Construction of factories, movie theaters, shopping malls, and especially large garages necessitates the use of slabs, which are a critical element of any project. Due to the huge expanses required by all of these constructions and the unavailability of close columns, massive reinforcing was needed, resulting wider columns and larger footing. As a result, there were many different types of slabs available, including Bubble deck, Polystyrene shapes. slab that is ribbed or waffled and Hallow slab [1]. In this chapter, some of the previous studies on the behavior of ribbed slabs, high-strength concrete, and strengthening with carbon fiber laminated plates or sheets will be reviewed.

2.2 Waffle slab or ribbed slab

The experimental and theoretical studies on reinforced concrete waffle or ribbed slab were rather limited, but here some of the researches were listed below;

An experiment was conducted in 2000 by **Abdul-Wahab and Khalil** [9] to look at how square waffle slab models behave, stiffen up, and ultimately hold up. Eight simply supported models (1540*1540mm size) and 150mm clear span with different rib spacing, slab depth, and two solid slab were tested to failure. The specimens were subjected to a central load over an area of 300*300mm. All of the experimental findings were compared to the

theoretical analyses of the two models the equivalent thickness idea and the suggested effective modulus method. They realized:

- ❖ As the number of ribs rises, or, to put it another way, as the distance between ribs reduces, the stiffness will increase and the deflection will decrease.
- ❖ The thinnest slab had the most deflection under stress.
- ❖ The overall carrying capacity appears to rise linearly as ribs are added.
- ❖ The mechanism of failure changed from flexural failure to sudden punching failure as the height of the ribs increased.
- ❖ The matching solid slab broke with a weight that was 60% less than a waffle slab.

Prasad, Chander and Ahuja[10] in 2005 did a theoretical study using grid or grillage analysis done by FORTRYAN 77 . Three groups of waffle slab with dimensional of (6*6), (7*7) and (8*8) m were designed with variation of ribs depth and number in order to achieve better load distribution without using shear reinforcement. All the groups had fixed minimum top slab thickness (65 mm).

- ❖ For group one (6*6) m; four depths were analysis (0.130,0.140,0.150,0.160) m. and they found that 0.130m depth was increase the maximum allowable deflection by 13% so 0.140m rib depth was used and decreased the deflection but increase the dead load. another solution was used by increase rib's number but that lead to exceed the bending moment capacity which lead to make the rib double reinforcement so increase the depth is better than increase rib's number, so five ribs with 0.140m depth was the best design.

- ❖ For group (7*7) m; four depths were used (0.160,0.180,0.200,0.220) m, the previous group's depths not stubble for this group. They found that; the usage 5 ribs don't meet the recommendation design with any depth, beside that usage 7&9 ribs lead to increase the depth to 0.220m that's mean used double reinforcement so, nine ribs with 0.200 mm depth was the best design.
- ❖ For group (8*8) m; for depth were used (0.200,0.220,0.240,0.260) m, the best design was nine ribs with 0.240m depth.

R. Shabbar, N. Noordin in 2010[11] were made a comparison between solid slab made of regular concrete and one-way ribbed built of lightweight foam concrete The ratio of cement, sand, and foam utilized in the mix was 1:1:0.45, and the material was evaluated in the lab for flow, density, and compression. They employ ESTEEM Software, which was created to British standards, to figure out how much concrete, steel, and formwork will be needed. In addition to being able to compute the raw cost and placement cost for the floor design, it can also provide drawings of the sections and the amount of shears, moments, and deflection. and they discovered:

- ❖ In multi-story buildings, foam concrete can be utilized in place of regular concrete.
- ❖ The cost of a two-way solid slab with a beam was higher than a one-way ribbed slab without a beam. The primary cause was the use of extra steel bar in the solid slab. In addition, the solid slab's steel formwork material is costlier than the ribbed.

A study was conducted in 2013 by **Schwetz., Gastal and Silva F [12]** to better understand the behavior of waffle slabs. They tried a full-scale waffle-slab that was intended to be the surface of a tennis court. In order to conduct the experiment, strain gauges were put in four slab locations at the top and

bottom surfaces to safeguard it. Strain gauges were added to the steel reinforcement, which was then coated in epoxy. The vertical displacements were measured as shown Figure 2-1 using a precise optical level, and Figure 2-2 depicts where these instruments were located. The slab underwent testing 63 days after curing. At the conclusion of each of the three loading steps, the displacement and strain were measured. The slab loading operation took 87 days to complete. The structure was analyzed using the SAP2000, and a comparison between the results of the experiment and the numerical analysis utilizing a grid matrix and finite elements was made, demonstrating that modeling using the grid matrix approach is particularly efficient as long as the moment of inertia is utilized with the real values and the stiff connections between the structural parts are left alone. While employing FE in the daily operations of design firms proved to be labor-intensive and challenging



Figure 2-1 show displacement measurement[12]

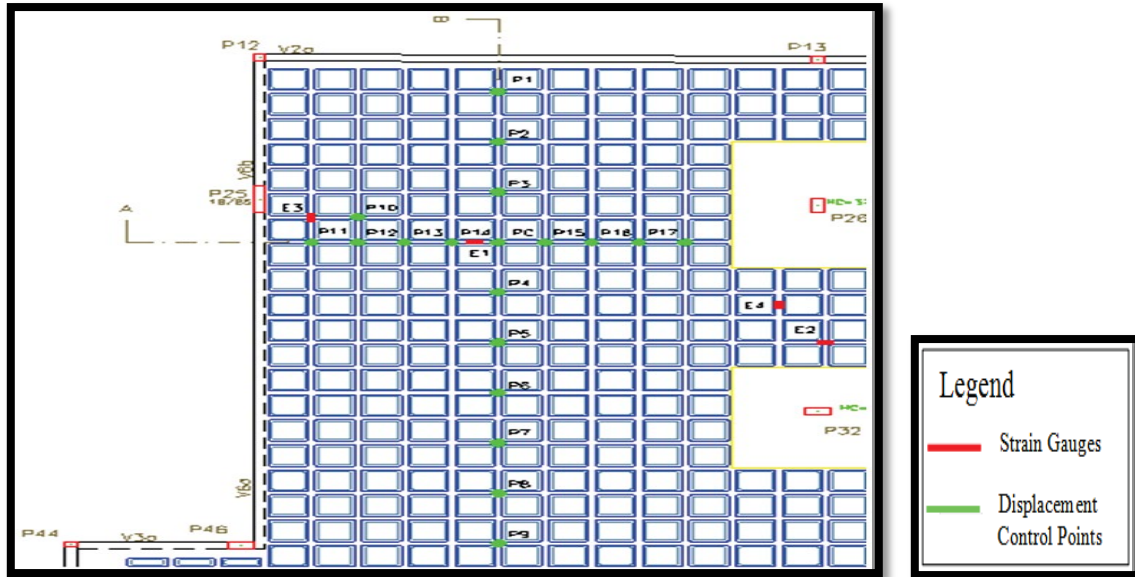


Figure 2-2 show the location of strain gauges and displacement control point [12].

Table 2-1 show details of tested specimens

Supported condition	Slabs thickness (mm)	Spacing between ribs in short span(mm)	Spacing between ribs in long span(mm)	Dimensions (mm)	Samples name
All four sides	40	-----	-----	300*900	S1
the short sides	40	-----	-----	1353*430	S2
All four sides	65	170	200	300*900	W1
The short sides	65	135	260	1353*430	W2

All the samples were tested under line concentrated load and they conclude that:

- ❖ The flexural moment of waffle slab for both small and large dimensions were higher than solid slabs by 22% and 33% respectively and the deflection in solid slab more than waffle slab because the waffles were stiffer that's due to the presence of ribs in tension zone so it was recommended to use waffle slab upon the solid slab in large span.
- ❖ The crack width at service load, was estimated and experimentally measured for both solid and waffle slab. the estimated crack width for waffle was higher than solid slab and that was the opposite of what found experimentally. The reason behind that was, on the estimation procedure took the waffle slab portion only which is smaller than solid slab, also it was based on ideal situations.
- ❖ At the end, the solid slab has higher deflection and lower flexural resistant compared with waffle slab. So it was recommended to used waffle slab upon the solid slab in large span.

Ahmad, Hashmi [14] in2017 Used steel fiber reinforced self-compacting concrete, there details listed in Table2-2. They examined the flexural and punched shear behavior of ribbed slabs (SFRSCC). Four ribbed slabs were cast, each measuring 2.8 meters long by 1.2 meters wide, with a total thickness of 0.2 meters. The height of the ribs was set at 0.1 meters for all slabs. Two of the samples underwent four-point bending (flexural) testing, while the third sample underwent punching sheer testing.

Table 2-2 Details of samples tested by Ahmad [14]

Samples design name	Reinforcement	Testing
CRC(F)	Conventional	Flexural
CRC(P)	Conventional	Punching shear
CFWS(F)	Full steel fiber	Flexural
SFWS(P)	Full steel fiber	Punching shear

The conclusion that they achieved was:

- ❖ SFWS ribbed slab samples under flexural stress delay the onset of the first crack, exhibited less ultimate load and lower deflection, and almost identical crack patterns to CRC.
- ❖ It was similar to a flexural test from deflection when the SFWS ribbed slab was subjected to punching shear, and the ultimate load was less than 27% of the CRC. The primary difference was in the manner of failure since the CRC had failed through punching-flexural mode. At the bottom of the slab, it was seen that the concrete cover started to split. Due to steel fiber bridging, the fracture on the bottom of the sample CFWS was more intact and had a lower breadth.

The flange served as the compression zone and the ribs as the tension zone at a positive moment. However, since the flange was thin, it would be tensioned in the adverse situation (on the support), thus it is crucial to harden this area, so **Sacramento , Picanço and Oliveira in 2018[15]** investigated how wide beams joining the columns may strengthen concrete structures, 4 square columns with widths of 200 and a thickness of 50 mm stand in the center of the slabs, two slabs were only supported by the x direction's edges putting load application in the middle (one-ways slabs) as shown in Figure2-3. The weight was applied at the four sides of the other two slabs, which were supported by a central column (two-way slab) were shown in Figure2-4, only in one direction was the ribs set. Each one is 80 mm broad and 100 mm high, joined together by a flange that is 50 mm thick. The broad beam depth's variance served as the primary factor. The dimensions of the broad beam were 150 mm, 200 mm, and 250 mm. the conclusions that they made;

- ❖ The findings of the experiments also showed that, in comparison to the slab without it, the stirrups in the ribs gave in even more ductile performance and decreased wide-beam displacements.
- ❖ The wide-beam-rib connection had a distinct cracking pattern compared to a flat slab, have wide longitudinal cracks running across its tensioned face.
- ❖ The computer study improved our comprehension of the behavior of either slabs, and showed that it wide-beam-rib connected experienced greater stress levels than the wide-beam column connection.

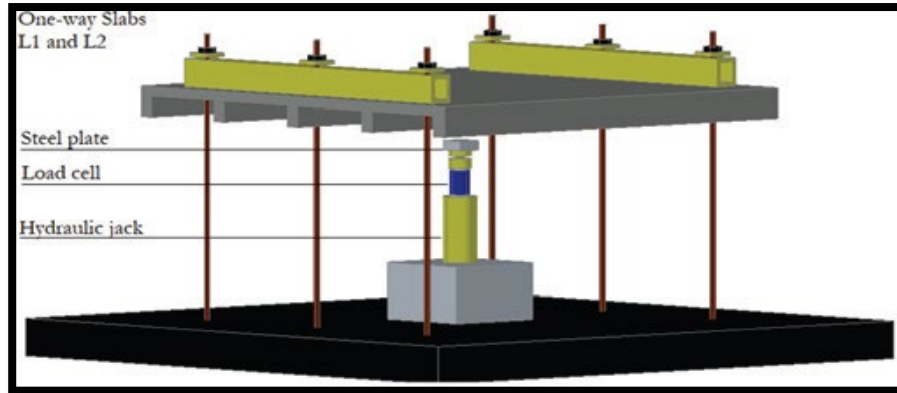


Figure 2-3 Test setup for one- way ribbed slab[15]

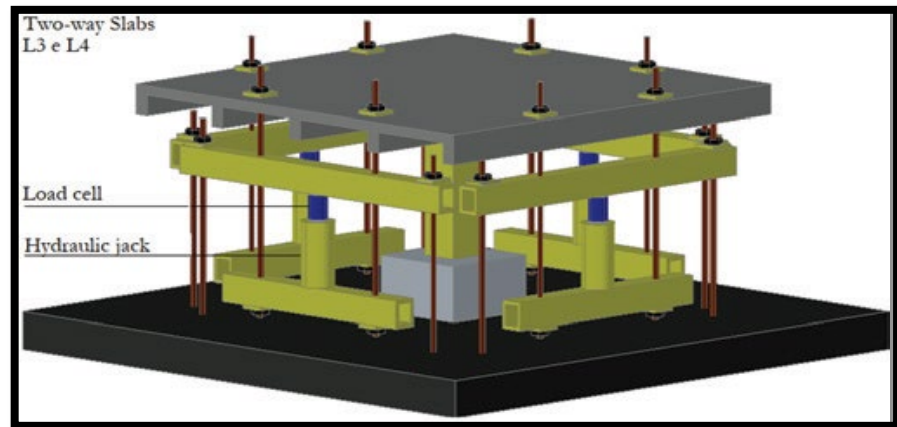


Figure 2-4 Test setup for two- way ribbed slab[15]

Mohammed and Kadhim[16] made a trial investigation in 2020 The experimental program includes analyzing the effects of replacing coarse aggregate (normal) with light aggregate (pumice stone) combined with and without steel fiber (volume fraction ($V_f = 0.25\%$)) on the strength and functionality behavior of HSNWC reinforced one-way ribbed slabs under dynamic and static loading. As part of the experimental investigation, 6 one-way ribbed slabs with 2 m in length, 0.9 m in width, and 0.150 m in depth were cast and tested. The ribbed slab samples were tested using a hydraulic testing equipment at the lab of civil engineering at Babylon University. Under

two-point loads, all ribbed slabs with a 1.7m clear span were assessed as a simply supported slab. Steel plates have been positioned underneath the two-point loads and along the support in order to prevent stress concentration and local concrete crushing. The constant (static)load was applied inertly at a loaded rate of 0.05 kN/sec up until the failure. They discovered:

- ❖ Using HSLWC in place of HSNWC in slab decreased the ultimate and cracking loads by 44.4% and 17.70%, respectively.
- ❖ The inclusion of steel fiber increased the HSLWC slab's ultimate load capacity and ability to remain free crack by 11.16% and 14.49%, respectively.
- ❖ The ductility of ribbed slab was reduced by approximately 4.75% until steel fiber was added.
- ❖ All ribbed slab specimens had hardness indices I5 and I10 that are greater than the typical values of 5, 10, and 20, respectively. The toughness index values showed that every slab's behavioral pattern is quite close to be in plastic state.

2.3 Strengthening with CFRP.

There is a societal demand for rehabilitation that is quickly expanding in order to address the problem of deteriorating infrastructure. A significant amount of infrastructure needed to be repaired or replaced as a result of increased population density, exposure to severe weather, and physical damage such (collision and impact). To assist with some of these problems, FRP has been used in civil engineering. CFRP sheets or laminates have drawn special interest for externally bonded strengthening purposes because of its

advantageous characteristics, including their low weight, high strength, stiffness, high durability, and simplicity of application[17].

Shahawy, Arockiasamy in 1995[18] examined Four rectangular beams made of reinforced concrete produced with the least amount of steel reinforcement. The beam had the following measurements: 203 mm broad, 305 mm deep, and 2744 mm long. Two steel reinforcing bars with a 13 mm diameter made up the flexural reinforcement (414 MPa minimum yield stress). The castings required conventional ready-mix concrete with a minimum compressive strength of 31MPa. The beams were given four weeks to cure before the CFRP strengthening was applied. Table 2-3 shows how many CFRP layers were put to each beam in total. The control beam utilized was specimen S5-STL. To repair the pre-stressed slab pieces, unidirectional (UD) CFRP tape was applied to the tension face of the concrete beams. The beams were put to the test with a basic span of 2,440 mm under four-point static stress. A hydraulic jack was used to apply the stresses at 0.152 m on either side of mid-span. They discovered

Table 2-3 details of tested beam[18]

Concrete compressive Strength (kN/m ²)	Number of CFRP layers	Beam Number
29,647		S5-STL
29,647	1	S5-PRE1
41,368	2	S6-PRE3
41,368	3	S6-PRE5

- ❖ The greater stiffness brought on by the laminate restraining effect is what is responsible for the increased first crack load for laminated beams. For the beam with one, two, or three CFRP layers, the proportional increase in the observed cracking moment was 12, 61, and 105, respectively.
 - ❖ The observed ultimate moment for laminated beams increases considerably as the number of CFRP layers increases.
 - ❖ Regard to more CFRP laminates, the deflection of the laminated beam shows a substantial decrease.
 - ❖ With more lamina, the strain on the concrete was significantly reduced.
- Ramana ,Kant in2000**[16] examine the various levels of beam strengthening. By adjusting the CFRPC laminate's width, the strengthened beams may be made to match below-reinforced, near balanced, as well as over reinforced parts. The three separate beam types listed above were manufactured utilizing 0.01, 0.02 and 0.04 m widths. Each type of beam's CFRPC laminate then converted to an equivalent amount of steel reinforcement to provide a measure of the proportion of balanced reinforcement. The proportion of balanced steel equivalent in beams reinforced is around 52% for 0.01 m width ,89% for 0.02 m width, and 142% for 0.04 m width. Four beams' sets, were tested in four-point bending across a span of 900 mm, one without CFRPC and three with varied degrees of CFRPC reinforcement by altering the width of the laminate. The beam had dimensions of 0.1 m in width, 0.1 m in depth, and 1 m in length, with 0.9m clear span they discovered:
- ❖ The first crack ultimate moments of strengthened beams were noticeably greater than those without CFRPC beams, demonstrating the reinforcing

impact of the CFRPC laminate. First crack and final moments both experienced increases of up to 150 and 230%, respectively.

- ❖ Reinforced beams become much more rigid, reaching a maximum stiffness of around 110percentage points with in case of an over-reinforced CFRPC. The deflections at failure load appear to diminish as the degree of strength increases. The ductility of reinforced beams has fallen as a result. Deflection criteria-based ductility ratios seem to be less advantageous than those based on curvature and energy.
- ❖ All reinforced beams failed by the typical CFRPC laminate peeling caused by flexural shear fractures. The reinforced beam had more fractures at the maximum load than a virgin beam, clearly demonstrating the composite activity of the CFRPC laminate.

Esfahani , Kianoush and Tajari in 2006 [3] looked at the flexural behavior of CFRP-sheet-enhanced reinforced concrete beams. They examined the impact of the reinforcing bar ratio (ρ) on the flexural of reinforced beams. Different specimens of CFRP sheets have different widths and layers counts. Twelve concrete beam samples measuring (150 mm*200 mm*2000 mm) were produced and put to the test. As references, three specimens weren't strengthened and maintained. The sample names were Ba-Bed-cLd. The numbers 1, 2, 3, and 4 stand for the number of beams, the diameter of the tensile bar, the number of layers, and the width of the CFRP sheet, respectively. With the exception of how many CFRP layers each of the specimens B2, B3, and B4 have, they are comparable. In these cases, the edges of a CFRP sheets were cut off 100 mm from the supports. The specimens tested under four- point load system. Also a theoretical analysis done according to ACI-440-2R-02 [20] and ISIS Canada [21]. The

displacement, ultimate load and type of failure are listed in Table 2-4. Type 1 flexural failure involves the crushing of compressive concrete, which may occur prior to or following the yield of reinforcement in tension zone; Type 2 FRP laminate's fracture follows the yielding of tensile steel; Type 3 end of FRP cover delamination.; and Type 4 FRP separation from the concrete surface. (4-b) debonding caused by a flexural crack; (4-c) debonding driven by a flexural-shear crack; (4-a) debonding of the plates' ends, type 5 failure due to shear.

Table 2-4 the test result[3]

Specimens (kN)	ρ	Ultimate load, P_u	P	P_u –	P_{u0} (mm)	P/P_{u0} (%) (mm)	Failure type ^a
B1-12D-0L	$0.3\rho_b$	P_{u0} 49.46	–	–	–	–	1
B2-12D-1L15		61.45	11.99			24	2
B3-12D-2L15		70.94	21.48			43	3
B4-12D-3L15		74.44	24.98			51	3
B5-16D-0L	$0.6\rho_b$	P_{u0} 75.94	–	–	–	–	1
B6-16D-1L10		84.93	8.99			12	2
B7-16D-1L15		94.92	18.98			25	2
B8-16D-2L15		105.91	29.97			39	2
B9-20D-0L	$0.8\rho_b$	P_{u0} 96.42	–	–	–	–	1
B10-20D-1L10		106.32	9.90			10	2
B11-20D-1L15		108.91	12.49			13	4-b
B12-20D-2L15		113.41	16.99			18	4-c

Finally, they stated:

- ❖ Similar to earlier investigations, the strengthening beams' flexural strength and stiffness increased in comparison to the reference sample.
- ❖ Testing results revealed that, when compared value of ρ max, the predictions made using ACI 440.2 and ISIS Canada overestimate the impact of CFRP sheets in enhancing the flexural strength of beams with lower reinforcing bar ratios.

- ❖ The ratios of the applied load to the load established by ACI 440.2 and ISIS Canada rise as the reinforcing bar ratios do. the calculations proposed by ACI 440 and ISIS Canada become progressively appropriate when the reinforcing bar ratio increases to the maximum value, mix.
- ❖ When ρ max, is reached, the reinforced beams fail with adequate ductility in either Type (4-b) or (c). In these kinds of failures, the CFRP sheet's reduced rigidity during the debonding process is to blame.

Abdulah in 2015[22] examined the different ways that CFRP sheet might be used to retrofit and reinforce one-way slabs. He examined nine samples, using a control slab that had not been strengthened. The strength of two samples was increased at two distinct locations (30&37.5mm in the long direction) (group 1). In addition to the earlier strips (group 2), the other two were reinforced with (100&120mm) in a short direction. Two samples were evaluated for the layer, and they were reinforced similarly to group 1 but with two layers instead of one. The latter two were retrofitted with 30 mm in the long direction after being loaded to 67.4% and 80.2% of ultimate load, respectively. Upon testing the slabs under a focused line load, he discovered;

- ❖ When compared to the control slab, the CFRP sheet increase the ultimate load by 8 to 64 percent.
- ❖ Using CFRP sheets for reinforcement increased stiffness, maximum load, fracture load, and decreased deflection.
- ❖ Instead of increasing thickness, it is preferable to increase CFRP width.
- ❖ Repairing slabs by CFRP sheet increased ultimate load almost equally to that of corresponding strength.

Murad in 2018 [23] Investigated how the flexural behavior of strengthening RC beams was affected by the orientation angle of CFRP sheets. Carbon fiber sheets were used to strengthen four beams, but not the control beam. Different CFRP sheet configurations were used, as seen in Figure 2-5. CFRP sheets with 0.5 m and 0.166 mm(width*thickness) he concluded that: -

- ❖ The orientation angle of CFRP sheets has a significant impact on the flexural strengthening of RC beams using CFRP sheets.
- ❖ The beam strengthened with 45 ° angle inclined Carbon fiber added 12percent more flexural strength than the control one, having the maximum measured flexural strength.
- ❖ The carbon fiber sheets' orientation angle significantly affects the fracture pattern and, in turn, the failure mechanism. Samples' F-45 and F-60 collapsed due to the development of a significant tensile-flexural fracture, whereas beams F-0 and F-90 failed due to the development of a significant shear-flexural crack.
- ❖ It is advantageous to use 45-degree inclined CFRP sheets to obliquely reinforce RC beams. The highest performing beam was Beam F-45, Strength and deflection both increased by 12percent & 56percent, respectively. While seeing 8percent reduction in ductility.

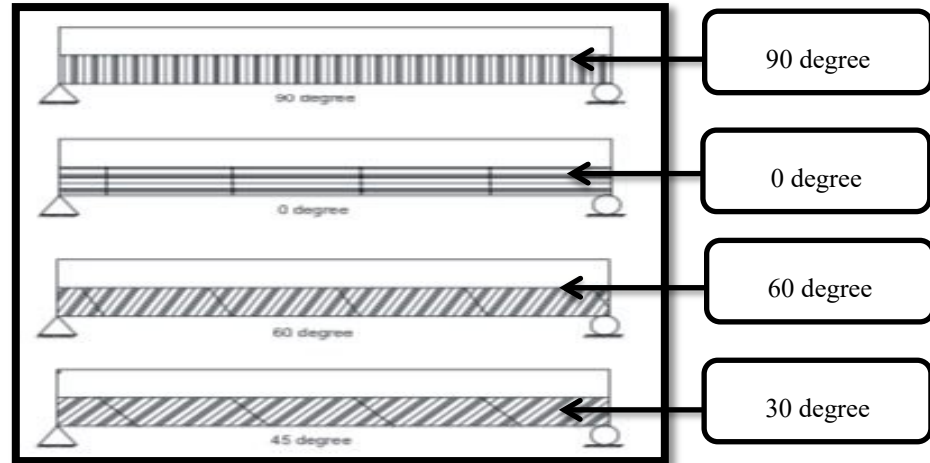


Figure 2-5: Details OF beam strengthening with CFRP sheet[20]

Mahmoud, Hawileh and Abdalla in 2021[24] analyzed the behavior of RC structure that is 100 mm thick and has a 70 MPa compressive strength. 18 slab specimens in all were tested till failure with two-point loading. Depending on their steel reinforcement ratio (ρ), the samples were split into three groups. Three of the six samples in each set were the originals, while the other three were checked to ensure repeatability. The reinforcement ratios that were looked at were 0.45, 1.00, and 1.79%. One or two layers of CFRP laminates were used to strengthen four samples from each group. Additionally, two unstrengthen control specimens used as benchmark specimens in each group. The conclusion they made that:

- ❖ The reference specimen frequently displays the greatest deflection and, hence, the greatest ductility among all groups.
- ❖ In all strengthening situations, slabs have shown a higher percentage of load increase when two sheets are attached to the slab's soffits because the specimen's width is relatively wider than its depth and the two rebar are inadequate to bear all applied loads.

- ❖ steel's strain reaction demonstrates a comparable response while transitioning from the elastic to the inelastic zone before diverging as a result of the varied arrangements and configurations of the CFRP strengthening.
- ❖ Although not all of the strengthened specimens achieved the debonding strain, they all demonstrated brittle failure mode.
- ❖ The ultimate strain in the concrete at the top grows as the reinforcement ratio rises.
- ❖ It should be noted that in the C70 group, group when the reinforcement ratio was a minimum with single and double layer strengthening had the highest observed ultimate ductility.
- ❖ Since this group uses the most materials of any group in the C70 group, it is noteworthy that the behavior of toughness in the low reinforcement group is the greatest.
- ❖ Regarding how the reinforcement ratio affects C70, it is clear that as the reinforcement ratio increases, the contribution of CFRP reduces and eventually becomes constant at high reinforcement ratios.
- ❖ When the contribution of CFRP increased with a low reinforcement ratio group, the flexural capacity peaked when the compressive strength of concrete reached 70 MPa.

2.4 Summery

In the previous studies mentioned before, much research had been done to study the behavior of one-way ribbed slabs. They studied the flexural strength and how it was affected by the number of ribs and the spacing between ribs.

Special attention was paid to reduce slab weight by using light weight concrete. But there is a leak with using high strength concrete instead of NC or light-weight concrete. Strengthening structures with CFRP sheets was a common method, and many studies theoretically and/or experimentally analyzed structures such as beams, deep beams, solid slabs, and columns in shear and flexure in various ways.

CHAPTER THREE
EXPERIMENTAL PROGRAM

Chapter Three

3 Experimental Program

3.1 Introduction

The current research work was adopted to help understanding the flexural behavior of reinforced height-strengthened concrete one-way ribbed slabs strengthened with externally bonded carbon fiber reinforced polymer sheets (CFRP). Twelve specimens of RC slab were tested experimentally to investigate the deflections, cracks, as well as failure modes and ultimate load. The experimental program also includes testing of cubes, cylinders, and prisms, in addition to some building construction materials, to determine concrete's mechanical properties. The experimental program was presented in this chapter in a format that followed the practical procedures of construction and testing. Beyond that, the slab requirements, test preparation, test setup, and process are described in detail. Furthermore, the general instrumentation is explained, as well as the material properties.

3.2 Specimens Description

The aim of this research is to study the flexural behavior of ribbed slabs strengthen with CFRP sheets and cast them with high-strength concrete. Twelve specimens with same dimension (600mm) in width, 2000mm(length) with 140mm depth of ribs and 60 mm thickness of the slab over the ribs, all the dimension and steel reinforcement details were shown in Figure3-2. The specimens were distributed on three

groups. The first group contains two specimens (NC and HC) without strengthening as control, the second group (HCS-L1R50, HCSS-L1R50, HCSS-L1R100, HCL1-WR), the third group (HCS-L2R50, HCSS-L2R100, HCSS-L2R50, HCSS-L2R100, HCSS-L2R100, HCS-L2WR) were shown in Figure 3-3 and their details listed in Table 3-1.

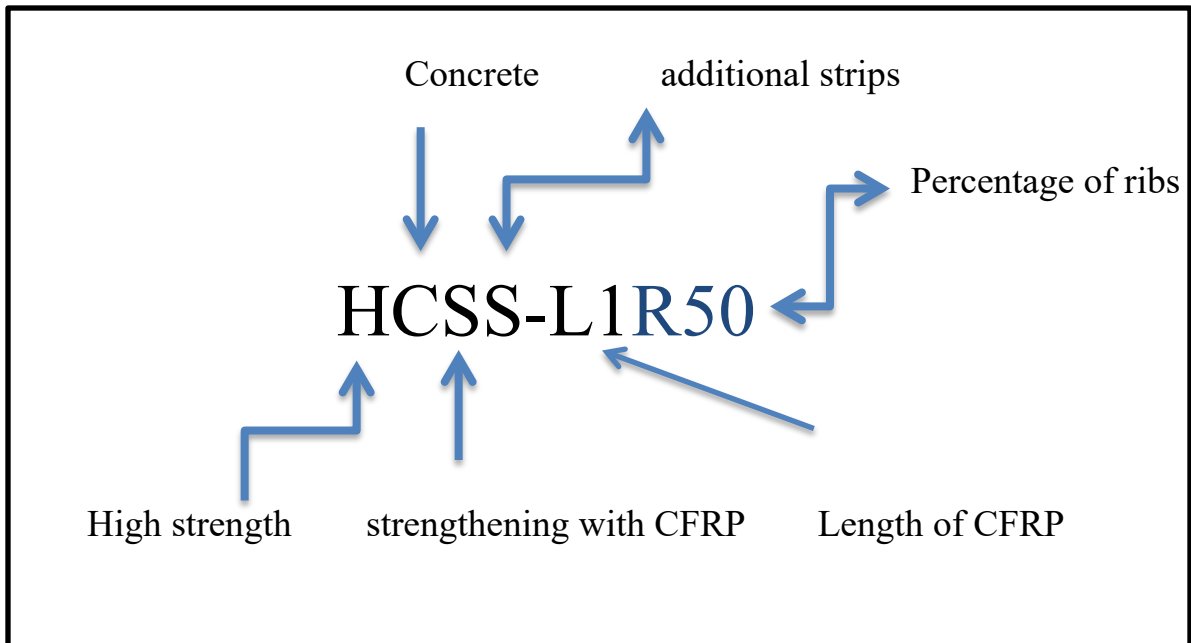


Figure 3-1 Definition of description specimens name.

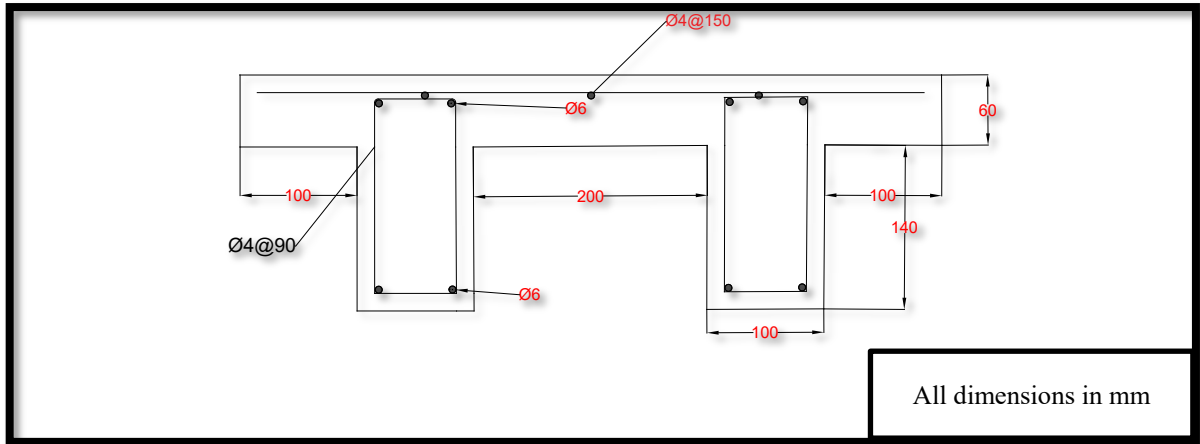


Figure 3-2 The dimension and steel reinforcement of all tested ribbed slab.

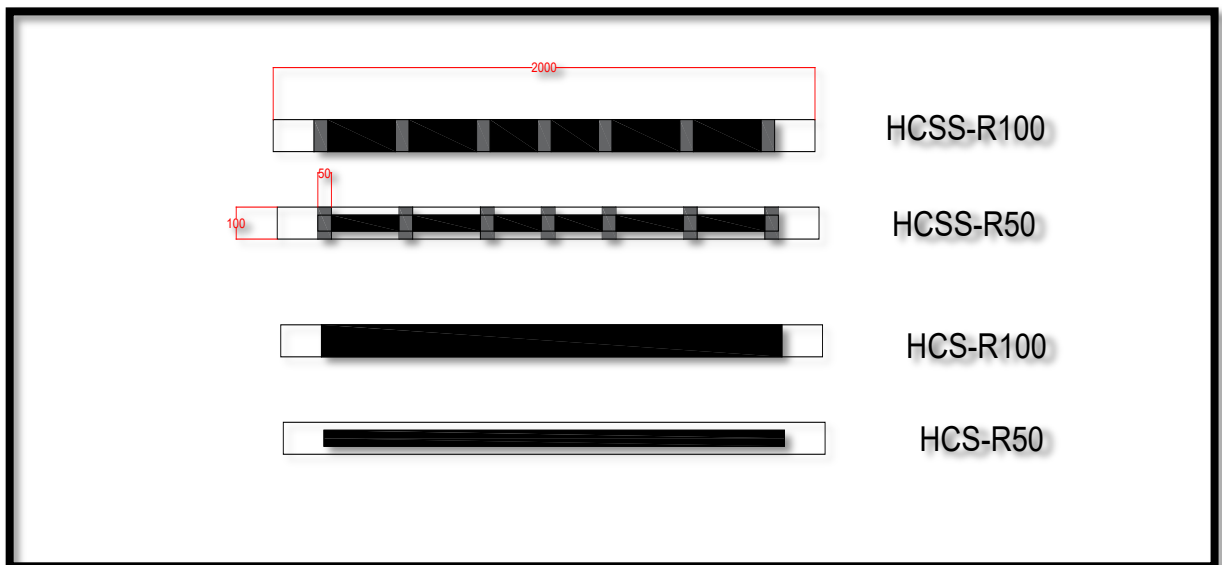


Figure 3-3 Ribs' bottom of group three specimens.

Table 3-1 Details of all tested groups' specimens.

Group No.	Length of strengthening	Design name	Details
Group 1	/	NC	Normal concrete without strengthening
		HC	High strength concrete without strengthening
Group 2	1250mm	HCS-L1R50	HSC with 50mm width of CFPS in each rib
		HCSS-L1R50	HSC with 50mm width of CFPS in each rib & 50mm U-shaped strips @250mm
		HCS-L1R100	HSC with 100 mm width of CFPS in each rib
		HCSS-L1R100	HSC with 100mm width CFRP in each rib &50mm U-shaped strips @250mm
		HCS-L1WR	HSC with strengthening all ribs
Group 3	1700mm	HCS-L2R50	HSC with 50mm width of CFRP in each rib
		HCSS-L2R50	HSC with 50mm width of CFPS in each rib & 50mm U-shaped strips @250mm
		HCS-L2R100	HSC with 100 mm width of CFPS in each rib
		HCSS-L2R100	HSC with 100mm width CFRP in each rib &50mm U-shaped strips @250mm
		HCS-L2WR	HSC with strengthening whole ribs

3.3 Specimens Preparation

This part includes reinforcement cages and mold preparation, mix design, mixing procedure, casting, curing and strengthening of the specimens.

3.3.1 Reinforcement Cages

One sizes of deformed steel reinforcement bars is used to manufacture the reinforcement cages for all specimens ⁽¹⁾. Steel bars of 6 mm diameter are used as longitudinal reinforcement, and steel bars of 4 mm diameter is used as shear reinforcement (stirrups) with rectangular close shape, also steel bars of 6mm are used to hold the stirrups in compression zone. For shrinkage and temperature requirements 5 mm mesh at 150 mm is used. Figure 3-4 shows cage of steel reinforcement.



Figure 3-4 Steel reinforcement preparation.

3.3.2 Mold Preparation

To accommodate the reinforcement cages, four plywood molds were built. The mold was made to be reused without causing damage to the slab or plywood. As a result, cork was utilized at the opening between the ribs in the dimensions of 200 x 140 mm, and it will be removed later. Before casting, the molds were oiled and placed on a horizontal level. Following this, the cages are installed, and 15 mm plastic spacers are utilized to achieve cover on the sides and bottom. Mesh is then placed on the ribs and fastened with thin steel wire. Figure 3-5 shows mold Preparation.

(1) The specimens reinforced with minimum reinforcement requirement of ACI 318-19 .



Figure 3-5 Mold preparation for casting and steel reinforcement installation.

3.3.3 Mix Design

The slabs were cast using two different mix designs. One was Normal-strength concrete with a compressive strength of 30 MPa after 28 days, and the other was high-strength concrete with a 28-day compressive strength of 60MPa. The high-strength concrete mix had been chosen from [Al-awiady, 2023[25] with a modification on W/C ratio and it was (1 cement: 1.31 sand: 1.93 gravel, by weight). Table 3-2 shows the mixture proportions (by weight) of the selected concrete mix.

Table 3-2 mix design percentage for both NC and HSC.

Material	Normal concrete	High strength concrete
Cement	400	550
Sand	700	720
Gravel	1056	1060
Water/cement	0.52	0.22
Silica fume	–	70
Super plasticizer	–	2.5/100 of cement

3.3.4 Mixing Procedure, Casting and Curing.

The specimens were cast in four separate days; two batches of concrete were used to cast each slab. A special shear mixer with a 350 kg capacity is used to mix the concrete. Before casting, the materials were prepared as shown in Figure 3-6. The sand and gravel were washed and sifted in sieve numbers (3 and 10) in the order and let them dry in the sun. After that, they were weighted as the mix required and packed in clean bags. In every batch, first mix the sand and gravel with a quarter amount of water and then blend them together. After that, cement and silica were added. The super plasticizer was mixed with the remaining water and added to the mix and allowed to remain in the mixer for a while. The mix was then cast in the molds that were oiled and compacted with a mechanical vibrator (1600 watts). On the first day of casting, three cubes of (100*100*100) mm dimension, three stander prisms (100*100*400) mm, and three cylinders (100*200) mm were cast to determine the concrete mechanical properties. On each day of casting, three cubes were cast. With the use of a steel trowel, the concrete's upper surface was leveled and finished



Figure 3-6 Mix preparing and casting.

After 24 hours of casting, all specimens were removed from the molds, and the slabs were covered with burlap bags to keep them moist for a further twenty-eight days. Cylinders, cubes, and prisms were placed in the curing water tank and kept wet in accordance with the standard specifications. After the curing, all the cork was removed and the surface smoothed to make the specimens ready to be strengthened as shown in Figure 3-7.



Figure 3-7 Curing and preparing samples for strengthening.

3.3.5 Strengthening of The Specimens

- ❖ Clean the surface from dust.
- ❖ The carbon fiber sheet was cut to the required length. (The tape was used to avoid shredded of CFRP sheets).
- ❖ Point the required place on ribs, where the CFRP sheet placing later.
- ❖ Using an electric mixer, the two partial compensations A (white) & B (black) of both the adhesive were merged in a ratio of 4:1 in accordance with the manufacturing (appendix A). The adhesive paste was then spread onto the concrete ribs surface with a brush till the color had been a consistent gray.
- ❖ Install the CFRP and make the epoxy saturated through it used a special roller for that let it dry for one day and put the second layer (stirrup)
- ❖ Let all the specimens dry for seven days. Figure 3-8 show the strengthening procedure.



Figure 3-8 Strengthening procedure from applying the adhesive and pointing the required CFRP places and installing the CFRP.

3.4 Material Properties

3.4.1.1 Concrete

It is a composite material composed of fine and coarse aggregate with cement that harden in the time.

3.4.1.2 Cement

All specimens are cast with Iraqi-manufactured ordinary Portland cement by Mass (an Iraqi company). Its chemical composition and physical properties are supplied by the manufacturer and compared with Iraqi specification [26] as given in Table 3-3 and Table 3-4 respectively.

Table 3-3 The chemical analysis and main components in cement.

<i>Item</i>	<i>Test Result (%)</i>	<i>Limits of Iraqi specification No.5/1984</i>	
<i>SiO₂</i>	20.88	-	
<i>Al₂O₃</i>	4.06	-	
<i>Fe₂O₃</i>	5.40	-	
<i>CaO</i>	62.41	-	
<i>MgO</i>	1.6	≤ 5.0%	
<i>SO₃</i>	1.19	≤ 2.8%	
<i>L.O.I</i>	2.86	≤ 4.0%	
<i>I.R</i>	0.56	≤ 1.5%	
<i>L.S.F</i>	0.91	0.66-1.02	
<i>Tri-calcium silicate</i>	<i>C₃S</i>	53.57	-
<i>Di-calcium silicate</i>	<i>C₂S</i>	19.45	-
<i>Tri-calcium aluminate</i>	<i>C₃A</i>	1.62	-
<i>Tetra-calcium aluminate ferrite</i>	<i>C₄AF</i>	16.43	-

Table 3-4 The physical analysis of cement.

<i>Item</i>	<i>Test Result</i>	<i>Iraqi specification No. 5/1984</i>
<i>Blaine fineness (m²/kg)</i>	326	≥ 230
<i>Compressive Strength (MPa)3 days</i>	20.33	≥ 20
<i>7 days</i>	28.0	≥ 23
<i>Time of setting (Vicat)Initial (hours: minutes)</i>	2:23	≥ 00:45
<i>Final (hours: minutes)</i>	3:25	≤ 10:00 hrs

3.4.1.3 Fine Aggregate

The fine aggregate for the entire project was natural river sand from Al-Ekhaider region. The results showed that the fine aggregate grading within zone 3 and the grading of the sand and sulfate content Figure3-9, as stated in Table 3-5 were in compliance related to the need for Iraqi specialization (IQS 45/1984)[27].



Figure 3-9 Test of SO₃ content in sand.

Table 3-5 Sieve analysis of fine aggregate and comparison with Iraqi specification.

sieve size	passing %	
	sand	Iraqi specification No.45/1984 with Zone two
10mm	100	100
4.75mm	100	90-100
2.36mm	94.85	85-100
1.18mm	86.6	75-100
600µm	70.11	60-79
300µm	38.15	12-40
150µm	7.22	0-10
SO3 contents=0.23% (specific requirements up to 0.5%)		
fineness modulus= 3.03		

3.4.1.4 Coarse Aggregate

The gravel used in the current study has a maximum size of 10 mm and is local. Table 3-6 displays the grading and properties of the coarse aggregate that satisfies the criteria of the Iraqi standard specification (IQ. S No. 45/1984). The test was done in the building materials lab of the University of Babylon.

Table 3-6 Sieve analysis for coarse aggregate .

Sieve size	passing%	
	coarse aggregate	Iraqi specification No.45/1984
12.5	100	90-100
10	94.44	90-100
9.5	94.44	75-100
4.75	4.04	0-10

3.4.1.5 Mixing Water

Lab water is used in the mixture and curing of the specimens as well as washing the sand and gravel.

3.4.1.6 Silica Fume

In this investigation, Master Roc MS 610 from BASF is utilized in cement weight at a ratio of 13%, which is within the dose range of 5 to 15%. Table3-7 below illustrates typical properties.

Table 3-7 Typical properties from manufactured.

Form	powder
Color	grey
Density	0.55-0.7Kg/l
Chloride	<0.1%

3.4.1.7 Super Plasticizer

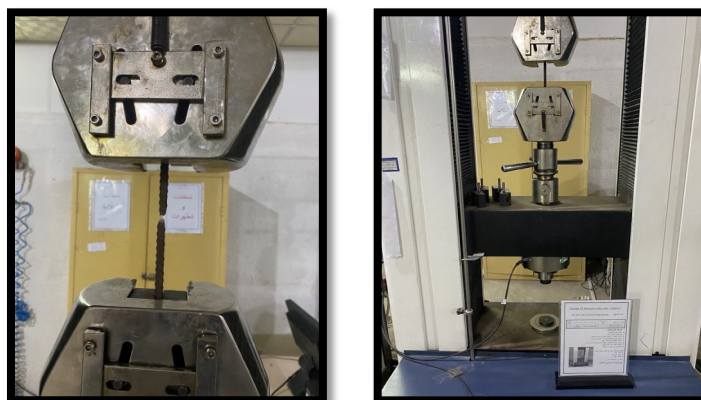
Master Glenium 54, which originates from Master Builders Solution's Dubai, United Arab Emirates plant and is classified by ASTM C-494 [28] as type F and G, BS EN 934-2 , and has the typical qualities listed in Table 3-8, is used as a plasticizer.

Table 3-8 Typical properties for super plasticizer

Form	Whitish to straw colored liquid
Relative density	1.07
PH	8-May

3.4.2 Reinforcing Steel Bar

In this study, two types of steel were used; ϕ 4 for stirrups and ϕ 6 in the tension and compression zones. The samples were examined in the material laboratory of Babylon University and Figure3-10 show the tested device, and Table 3-9 displays the reinforcing qualities.

**Figure 3-10 Steel tensile test.****Table 3-9 test result for steel reinforcing bars**

<i>Nominal diameter (mm)</i>	<i>Measured diameter (mm)</i>	<i>Area (mm²)</i>	<i>Yield stress (MPa)</i>	<i>Tensile strength (MPa)</i>	<i>elongation %</i>
6	5.1	20.42	500	620	7
4	3.92	12.06	420	500	4

The type of CFRP sheet utilized to reinforce the slabs was (Sika Wrap Hex-230C). The characteristics of it depicted in Appendix B.

3.4.3 Epoxy

Sikadur-330 is used to adhesive carbon fiber sheet with concrete. It is composed of two parts (Resin part A and hardener part B).

3.5 Harden Concretes Test

3.5.1 Compressive Strength

Twelve 100*100*100 mm cubes and three 150*150*150 mm cubes were examined using automatic compression device with a 2000 kN capacity as part of tests conducted at Babylon University's structural laboratories as shown in Figure 3-11 in accordance with British Standard BS1881-part 116:1989[29].

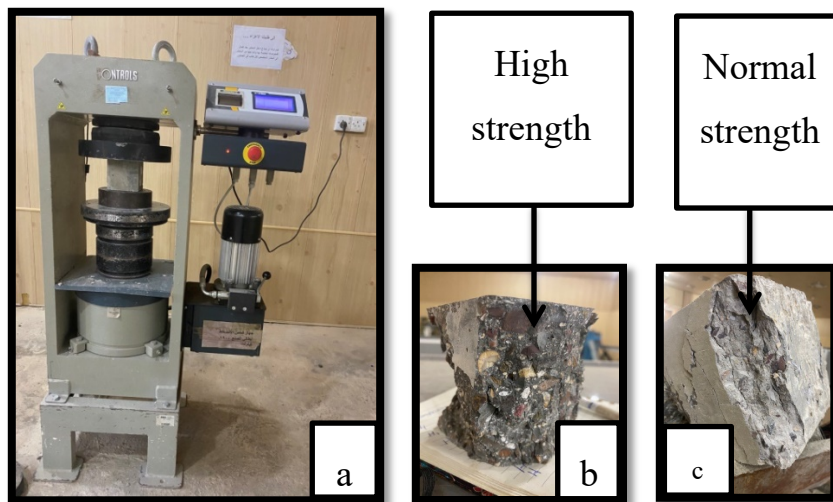


Figure 3-11 Compressive strength test, {a} the compressive strength device,{b} compressive failure of HSC, {c} compressive failure of NC.

3.5.2 Tensile Strength

According to ASTM C496, 2011[30], splitting tensile stress tests were conducted at Babylon University's structural laboratories,Figure3-12, to

compute tensile stress indirectly. Six cylinders measuring (100*200 mm) were tested.

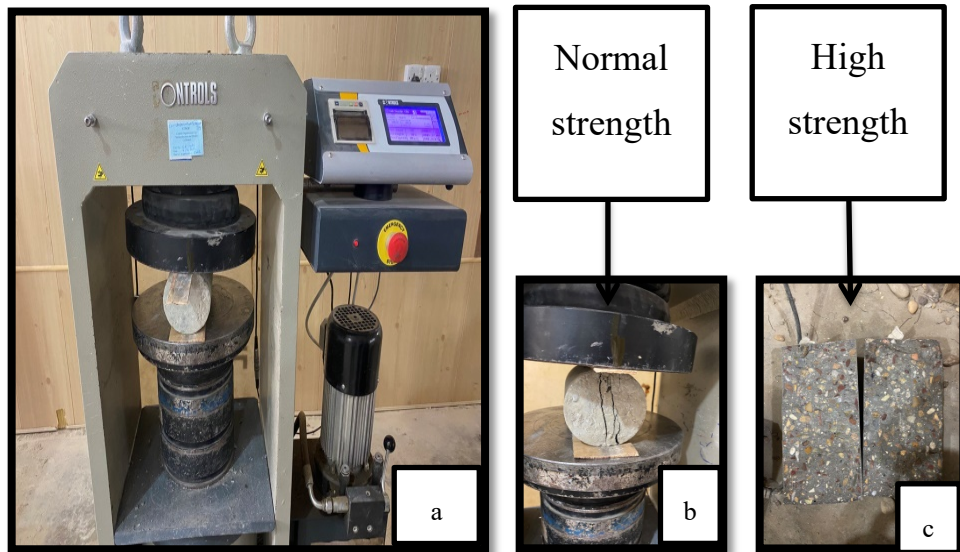


Figure 3-12 Split tensile test, {a} testing device, {b} tensile failure of NC, {c} tensile failure of HSC.

3.5.3 Modulus of Rupture

In the Structural Laboratory of the Civil Engineering Department at the University of Babylon, Figure3-13. A total of six concrete prisms measuring (100*100*400)mm were tested as small, simple supported beams under two concentrated loads as ASTM C78 standards requirement[31], utilizing a universal hydraulic machine with a 2000 KN maximum capacity.

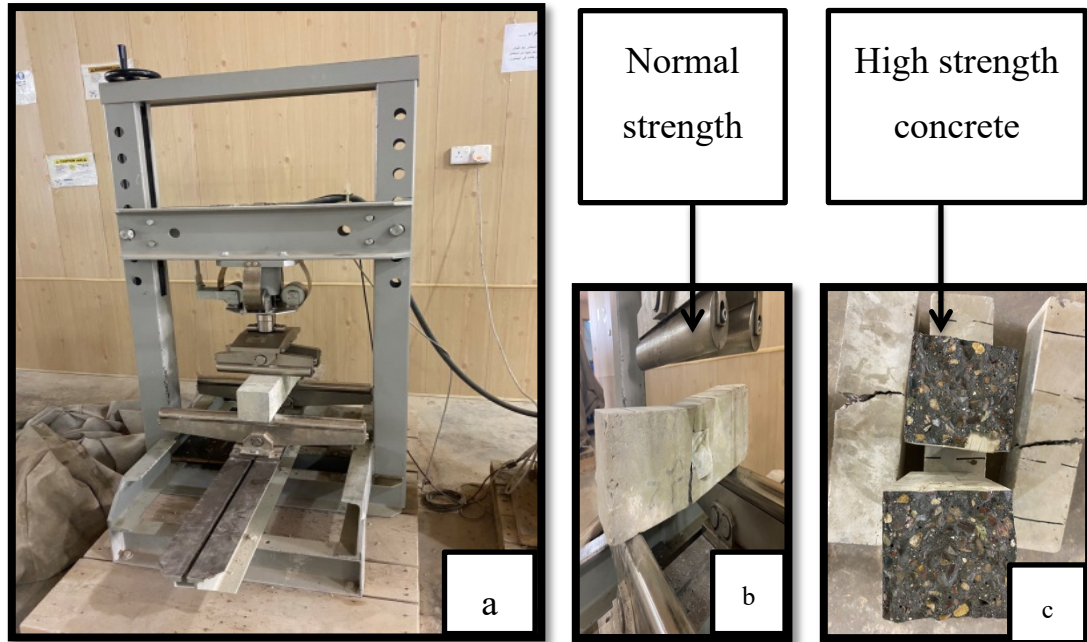


Figure 3-13 Modules of rupture test, {a} testing device, {b} flexural failure in NC, {C} flexural failure in HSC.

3.6 Test Instruments

3.6.1 Testing Machine

The behavior of ribbed slab was examined using the hydraulic testing device. A testing facility with a 600 kN capacity is located in the civil engineering laboratory at the University of Babylon as shown in Figure3-14.

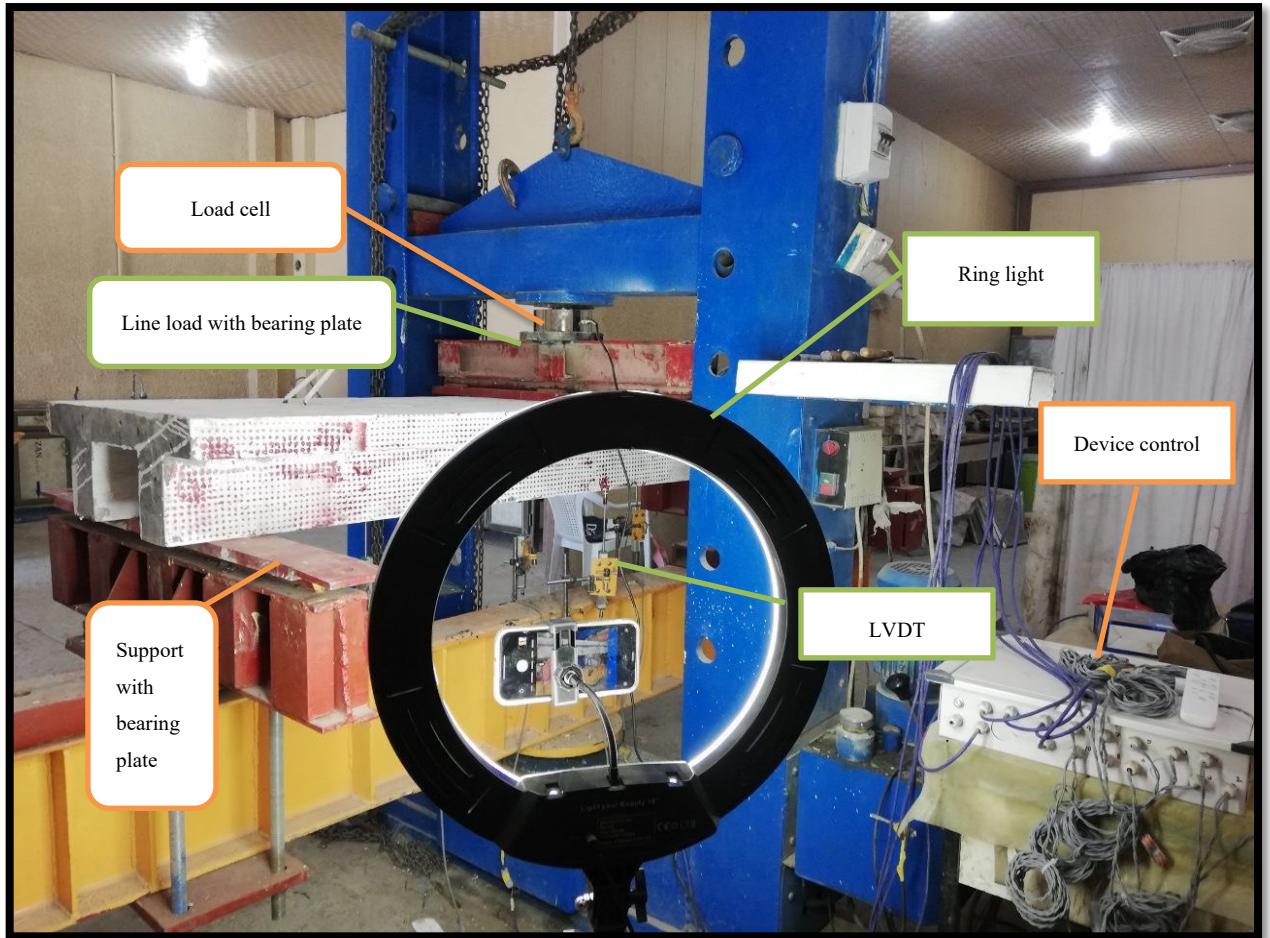


Figure 3-14 Full details of testing device.

3.6.2 Supporting and load conditions

One-way ribbed slab was tested as a simple supported beam, therefore one end was placed on a hinge and the other on roller support, Figure 3-15 show hinge and roller plates. The load was applied through a steel beam. A bearing steel plate was inserted at the support and load points to avoid concrete crushing.



Figure 3-15 supporting of specimens

3.6.3 LVDT

An electromechanical device known as a linearly varying differential transformers {LVDT} converts mechanical motion or vibrations—more especially, rectilinear displacement into a changeable electrical current, volts, or electrical signals. Four LVDTs were utilized in this work, one to compute deflection in the middle of the span, one for the third of the ribs, and the other two to verify the symmetry of the ribs, Figure3-16 show the LVDT position.



Figure 3-16 Position of LVDT.

3.7 Test procedure

Before the test began [Figure3-17], all the specimens were cleaned, painted white, tagged with their names, and moved to the university lab. At the test beginning, the supported was installed in horizontal position, then the ribbed-slab laying on it. Further, the places where the LVDT and load plate were pointed After that, connect the LVDT and the load cell to a data logger to collect the data that will be analyzed later. At each day of testing, three cubes were comprehensively tested.



Figure 3-17 Test procedure from transporting the specimens to installation of all the tested specimens.

CHAPTER FOUR
EXPERIMENTAL RESULT
AND
DISCUSSIONS

Chapter Four

4 Experimental Results and Discussions

4.1 Introduction

The most significant results from the experimental program mentioned in chapter three are summarized and analyzed in this chapter. First, as detailed in the final section of chapter three, the properties of hardened concrete as determined by tests on the control samples (cubes, cylinders, and prisms) are displayed. The test findings from the specimens are then shown and explained, including the ultimate load, modes of failure, responses of load deflection, stiffness, and results of cracking behavior.

4.2 Mechanical properties of concreteThe mechanical properties of the hardened concrete, which was used to cast all of the slabs specimens, are investigated in a number of experiments on the control samples (cubes, cylinders, and prisms) after the curing period. Each result is derived from the average of three samples. According to the results, which are displayed in Table [4-1], the experimental values are consistently greater than the theoretical ones provided by the ACI codes. Compressive, tensile and flexural tensile strength were provided from a laboratory test.

Table 4-1 show the concrete mechanical properties.

Concrete type	Cube Compressive Strength f_{cu} (MPa)	Cylinder Compressive Strength f_c' (MPa)	Splitting Tensile Strength (MPa)	flexural tensile Strength f_r (MPa)	Theoretical flexural tensile Strength f_r (MPa)	
Normal	Sample 1	42.32	33.856*	3.61	3.608	3.07 [#]
	Sample 2	36.19	28.952*	2.38	3.336	2.45 [#]
	Sample 3	41.19	32.952*	3.00	3.559	2.66 [#]
	average	39.9	31.92*	2.9967	3.501	2.7267 [#]
High strength	Sample 1	83.53	71.0005**	6.3	7.921	7.83 ^{##}
	Sample 2	78.63	66.8355**	6.0	7.685	6.84 ^{##}
	Sample 3	74.18	63.05 3**	4.96	7.4641	6.59 ^{##}
	average	79.447	66.96 3**	5.753	7.692	7.09 ^{##}

* $f_c' = 0.8 f_{cu}$ (MPa) according to (BS8110-1-97) [32]

** $f_c' = 0.85 f_{cu}$ (MPa) for high strength according to (ACI363R-10).....[7]

[#] $f_r = 0.62 \sqrt{f_c'}$ (MPa) according to (ACI 318-14) [33]

^{##} $f_r = 0.94 \sqrt{f_c'}$ (MPa) according to (ACI363R-10)[7]

4.3 Test result of the specimens.

As mentioned before that there was two control slabs and three groups that tested to flexural analysis the influence of strengthening high strength concrete with carbon fiber sheet in different width and length, with and without U shaped strips .in this chapter, the data of deflection and load will have collected from LVDT and load cell respectively. the data will analysis and both stiffness and ductility will compute.

4.3.1 Load- deflection curve and ultimate load

4.3.2 4.3.1 Group One

The control slabs have been tested as group one; generally, both of them show typical performance under concentrated load; it shows liner behavior before cracking, then change slope and remaining liner until it reach the yield point and change from linearity to non-linearity [34]. The HC has smaller deflection than the NC at service loads before cracks' appearance cause the HC spesecimen was stiffer than the NC specimen, with only a minor increase in ultimate load, as illustrated in Figure4-1. HC shows a 19% increment in ultimate load compared with NC, the failure of HC was gradual and show fairly large deflection cuase the specimenes was under reinforcement as concluded from Pam et al [35]

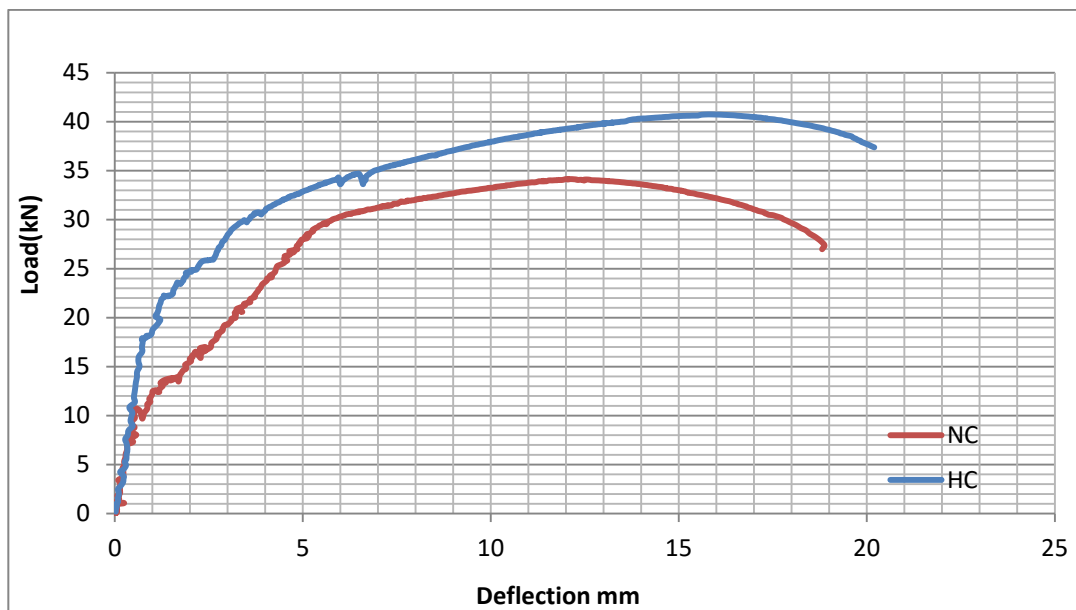


Figure 4-1 Load-deflection curve of group one.

4.3.2 Group Two

All specimens in this group, have been strengthened by carbon fiber sheet with a 1250mm length and different widths (50mm, 100mm,380mm), with 50mm additional U-shaped strips and without U-shaped strips. Unfortunately, one of the samples(HCSS-L1R50) was neglected due to a technical issue. The development strengthening length was calculated according to the prevent end peeling and debonding requirements in ACI440-2R-08 [36]. Its calculated from the equation below;

$$L_d = \sqrt{\frac{n t_f E_f}{\sqrt{f_c}}}$$

n ; number of CFRP sheets layer.

t_f ; CFRP sheets thickness.

E_f ; modulus of elasticity for CFRP

All the specimens are similar in elastic stage, but when the first crack appears, the specimens separate and show different behavior from the reference HC. The stage two in load-deflection curve, depends on stiffness. The results show the specimens with carbon fiber were stiffer than HC. That means the strengthened samples have less deflection at higher loads compared with HC because the CFRP wasn't a ductile material. The 100mm CFRP width, which is the same width as the rib, shows a 75% increase in ultimate load when compared to HC, while HCS-R50 shows 35% increment only. Generally; they show similar behavior and both were similar to specimens with strips in the region before failure. The specimens without strips Figure 4-3, when they reach ultimate load, the load begins to decrease rapidly and

linearly. While the samples with strips when reach ultimate load, it began to concave down (with the first CFRP sheet fracture) and return to an increase in load (concave up) until the sheet is no longer able to withstand extra load as shown in Figure4-2. It noted that the strips decrease the ultimate deflection and maybe, since the ribbed had minimum reinforcement and this percentage of width wasn't enough to rise the strength so CF reached nearly its tensile stress and failed by fracture. Besides that, the whole rib strength(380mm) behaves like samples with strips but shows a higher increase in ultimate load, reaching 133% from HC.

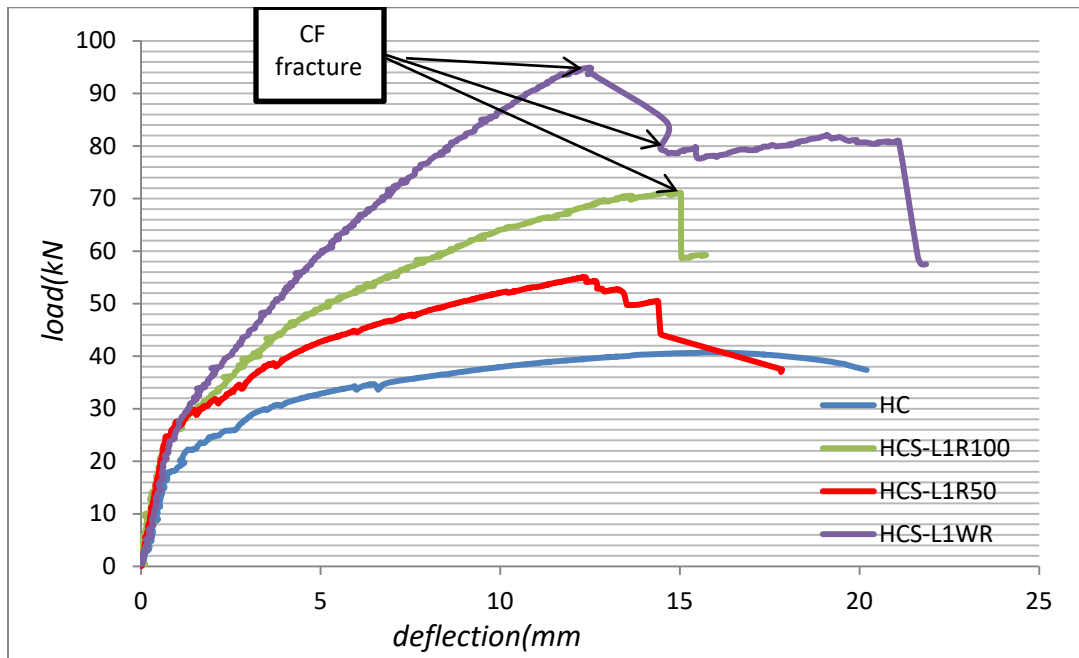


Figure 4-2 Group two, specimens without additional strips.

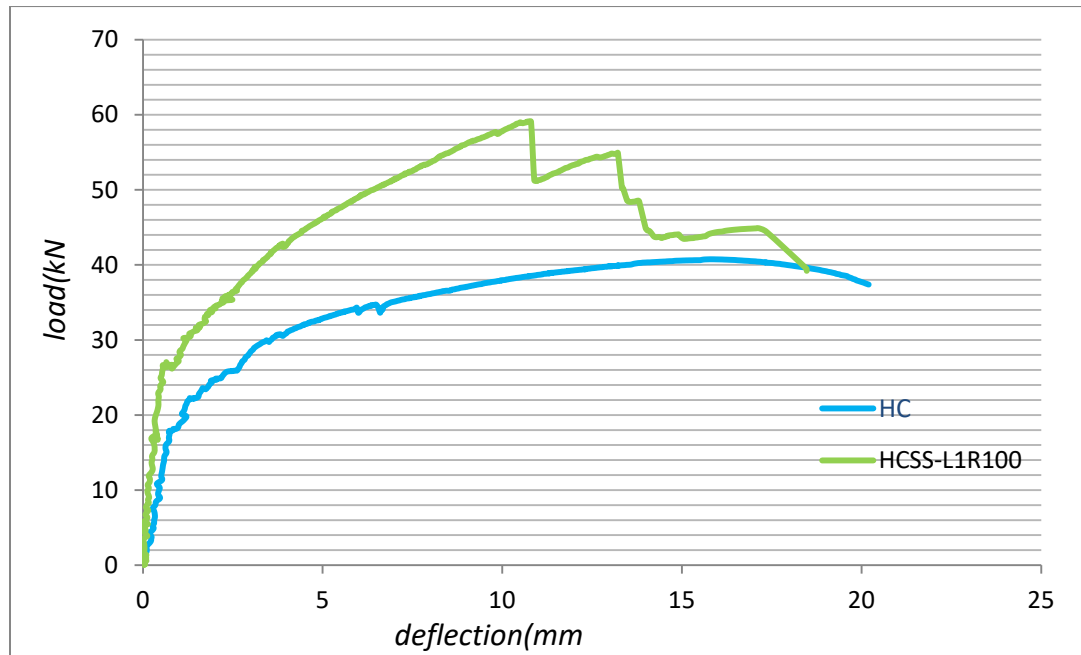


Figure 4-3 Load-mid span deflection for group two, specimens with additional U-shaped strips.

4.3.3 Group Three

This group is similar to group two but in 1700 mm length of sheet (clear span length). The load deflection curve was similar to group two with significant different just in value not in general behavior. The ultimate load for specimens HCS-R100, HCS-R50 had raised the ultimate load in 41%, 3% from HC respectively and this increment was less than the increment obtained from group two. In other hand, HCSS-R50, HCSS-R100, HCS-WR had raised the ultimate load in 18%, 73%, 167% respectively, and this increasement more than group one increasement. Figure 4-4, Figure 4-6 show the mid-span deflection vs applied load.

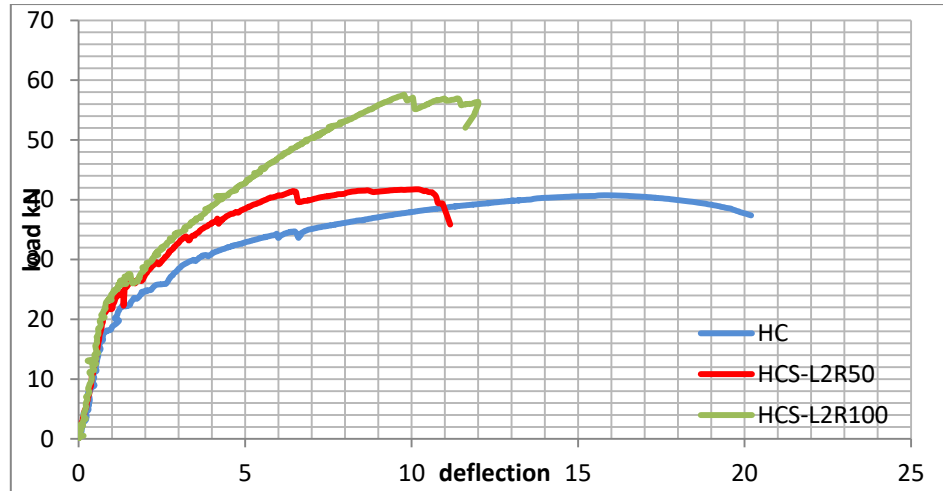


Figure 4-4 Load-mid-span deflection curve for group two to specimens without U-shaped strips.

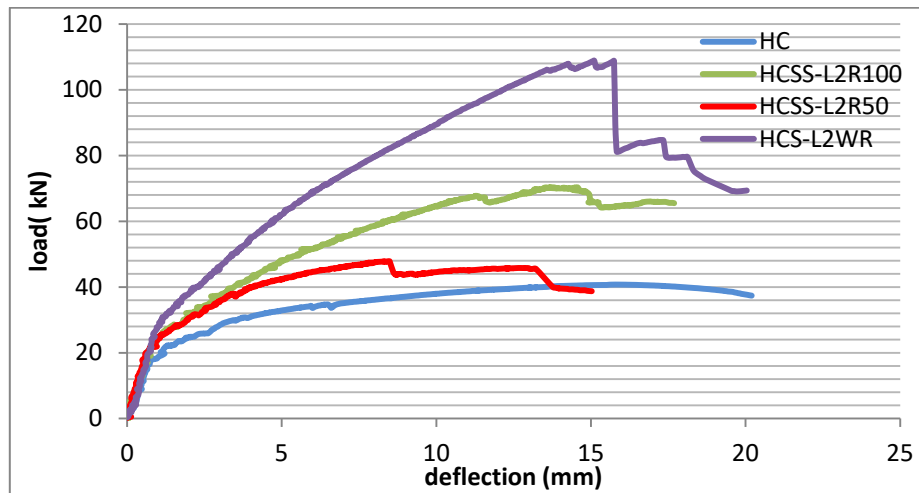


Figure 4-5 Load- mid span deflection curve for group two to specimens with U-shaped strips.

4.4 Stiffness

Stiffness is the criteria of load required for producing deformation and it has calculated from division 0.75% from ultimate load over 0.75% from ultimate deflection as required from [50]. Comparative between all tested specimens

from group two and group three with the HC specimen from group one was shown in Figure 4-6, and all the results obtained from the experimental work was listed in Table 4-2.

Table 4-2 Results obtained from the experimental work for all tested groups.

<i>Groups name</i>	<i>Specimens name</i>	<i>Ultimate load Pu (kN)</i>	<i>Increment in ultimate load (%)</i>	<i>Deflection at service load*, δ_s (mm)</i>	<i>Deflection at ultimate load, δ_u (mm)</i>	<i>stiffness K</i>	<i>Types of failure</i>
<i>Group one</i>	<i>NC</i>	<i>34.15</i>	<i>-16.00</i>	<i>3.21</i>	<i>12.00</i>	<i>5.68</i>	<i>Typical flexural failure</i>
	<i>HC</i>	<i>40.75</i>	<i>0.00</i>	<i>1.84</i>	<i>15.78</i>	<i>7.80</i>	
<i>Group two</i>	<i>HCS-L1R100</i>	<i>71.15</i>	<i>75.00</i>	<i>3.43</i>	<i>15.00</i>	<i>8.23</i>	<i>Rapture of CF sheet</i>
	<i>HCS-L1R50</i>	<i>55.04</i>	<i>35.00</i>	<i>2.37</i>	<i>12.33</i>	<i>9.17</i>	<i>Flexural failure without effecting the CF</i>
	<i>HCSS-L1R100</i>	<i>59.12</i>	<i>45.00</i>	<i>2.14</i>	<i>10.74</i>	<i>7.72</i>	<i>Cover delamination</i>
	<i>HCSS-L1R50</i>	<i>50.00</i>	<i>23.00</i>	<i>-</i>	<i>-</i>	<i>-</i>	<i>Flexural failure without effect the CF</i>
	<i>HCS-L1WR</i>	<i>94.87</i>	<i>133.00</i>	<i>4.30</i>	<i>12.53</i>	<i>10.26</i>	<i>Rapture of CF sheet</i>
<i>Group three</i>	<i>HCS-L2R100</i>	<i>57.58</i>	<i>41.00</i>	<i>2.86</i>	<i>9.78</i>	<i>8.48</i>	<i>Fracture of CF sheet</i>
	<i>HCS-L2R50</i>	<i>41.75</i>	<i>3.00</i>	<i>1.34</i>	<i>10.18</i>	<i>11.54</i>	<i>Flexural failure without effect the CF</i>
	<i>HCSS-L2R100</i>	<i>70.32</i>	<i>73.00</i>	<i>3.70</i>	<i>14.57</i>	<i>8.38</i>	<i>Cover delamination</i>
	<i>HCSS-L2R50</i>	<i>47.86</i>	<i>18.00</i>	<i>1.55</i>	<i>8.49</i>	<i>12.00</i>	<i>Debonding followed by CF fractured</i>
	<i>HCS-L2WR</i>	<i>108.84</i>	<i>167.00</i>	<i>5.35</i>	<i>15.11</i>	<i>9.78</i>	<i>Rapture of CF sheet</i>

*assume service load =ultimate load Pu /1.7.....[3]

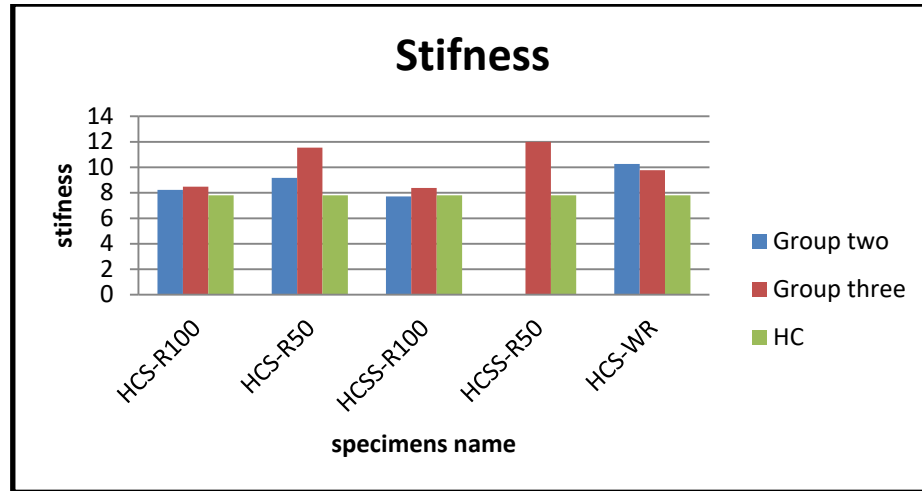


Figure 4-6 Comparative between stiffness for all groups.

4.5 Modes of failure.

There are many types of failure when RC strengthen with CFRP sheet such as debonding of CF sheet when CF U-shaped anchor haven't used, crushing of concrete, cover delamination, rupture of CF sheet and all these types of failure may occur before or after steel yielding [3]. In this study, for all tested specimens there is not any indication of CFRP failure except of a few popping precede the CF sheet rapture or fracture.

4.5.1 Group one

Both of HC and NC failed by flexural tensile steel yielding, the load still rising after the crack appearance to a certain limit then the load was dropped out. The ultimate load of HC was higher than NC.

4.5.2 Group two

This group can be divided into three sections depending on the type of strength, and failure and the entire failure mood were listed here:

✚ HCS-L1R50, when loading the specimen was started, the load keeps rising then the load was dropped off without crushing of concrete and any effect on the CF sheet and debond from the concrete when the load was decreasing as shown in Figure4-7. Since the specimen reinforced with minimum steel reinforcement ($2\Phi 6$ for each rib), it was possible to failed by steel yielding followed by debonding. While HCS-L1R100 was failed by rapture of CF sheet in the area under the line load[Figure4-8]



Figure 4-7 Type of failure on HCS-L1R50, steel yielding follow by CF sheet debonding.



Figure 4-8 Rapture of CF sheet on HCS-L1R100



Figure 4-11 CF sheet raptured on HCS-L1WR

4.5.3 Group three

In this group there are four modes of failure

- ✚ First: steel yielding without significant effect on the CFRP sheet in the HCS-L2R50 specimen[Figure4-12]



Figure 4-12 Flexural failure on HCS-L2R50.

- ✚ Second: fracture in carbon sheet due to shear crack directly in the zone under point load like HCS-L2R100 as shown in Figure4-13.



Figure 4-13 Flexural failure on HCS-L2R100 by CFRP fractured.

- ✚ Third: fractured in CFRP led to debond the CFRP sheet under point load in the area between two strips due to flexural crack but the strips prevent the CF sheet from separation until the CFRP reach its maximum stress as HCSS-L2R50(figure4-14).



Figure 4-14 Flexural failure on HCSS-L2R50 by fractured of CF sheet

- ✦ Fourth: failed by concrete cover delamination due to flexural-shear crack under point load such as HCSS-L2R100, it started with inclined crack in the concrete cover and extended along the tensile reinforcement[Figure4-15].

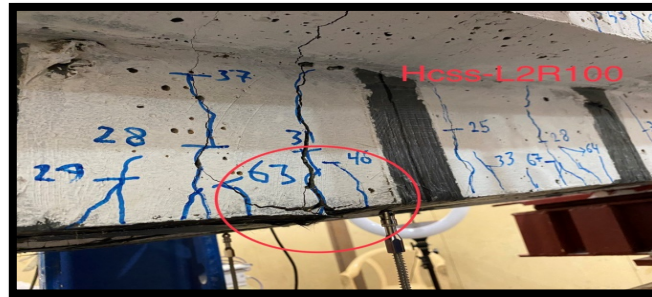


Figure 4-15 failure on HCSS-L2R100

- ✦ Fifth, the CFRP sheet rapture under point load in the bottom and sides of the ribs as same as HCS-L1WR as shown in Figure4-16.



Figure 4-16 Rapture of CF sheet on HCS-L2WR

4.6 Crack pattern

4.6.1 Group one

First crack was flexural and appeared in the middle zone of ribs, and the crack kept appearing under concentrated load and covering approximately the one – third or less of middle zone of ribs. Then when the load increase the cracks stopped appearing and the once that already exist were widening and lengthening through the ribs, fewer of them reach the slab. the cracks are symmetry in both ribs and they lengthening towards each other, so it could saw like one tall crack from bottom side. Figure 4-17 explained the cracks pattern of this group.



Figure 4-17 Cracks pattern of group's one specimens.

Table 4-3 show the first crack-load.

<i>specimens name</i>	<i>P_u(KN)</i>	<i>P_c(KN)</i>	<i>P_c/P_U%</i>
NC	34.14	10	29%
HC	40.75	18	44%
HCS-L1R100	71.15	23	32%
HCSS-L1R50	50	24	48%
HCSS-L1R100	59.12	28	47%
HCS-L1R50	55.04	26	47%
HCS-L1WR	94.87	75	79%
HCS-L2R100	57.58	25	43%
HCS-L2R50	41.75	22	53%
HCSS-L2R100	70.32	24	34%
HCSS-L2R50	47.86	11	23%
HCS-L2WR	108.84	73	67%

4.6.2 Group two

For all specimen the first crack was flexural and appeared in the middle of ribs but at deferent load. For both HCS-L1R50 and HCS –L1R100, all the cracks were flexural and covered the middle one –third of ribs, covering more area compared with the references(HC) while for HCSS-L1R50 and HCSS-L1R100, the cracks are fewer from the references and covered approximately one- fourth of the middle ribs area between the strips but most crack reach the slab cause the neutral axis would raise, and it is worth to mention that HCSS-L1R100 failed with flexural-shear crack. Figure4-18 shows the crack pattern for group two.

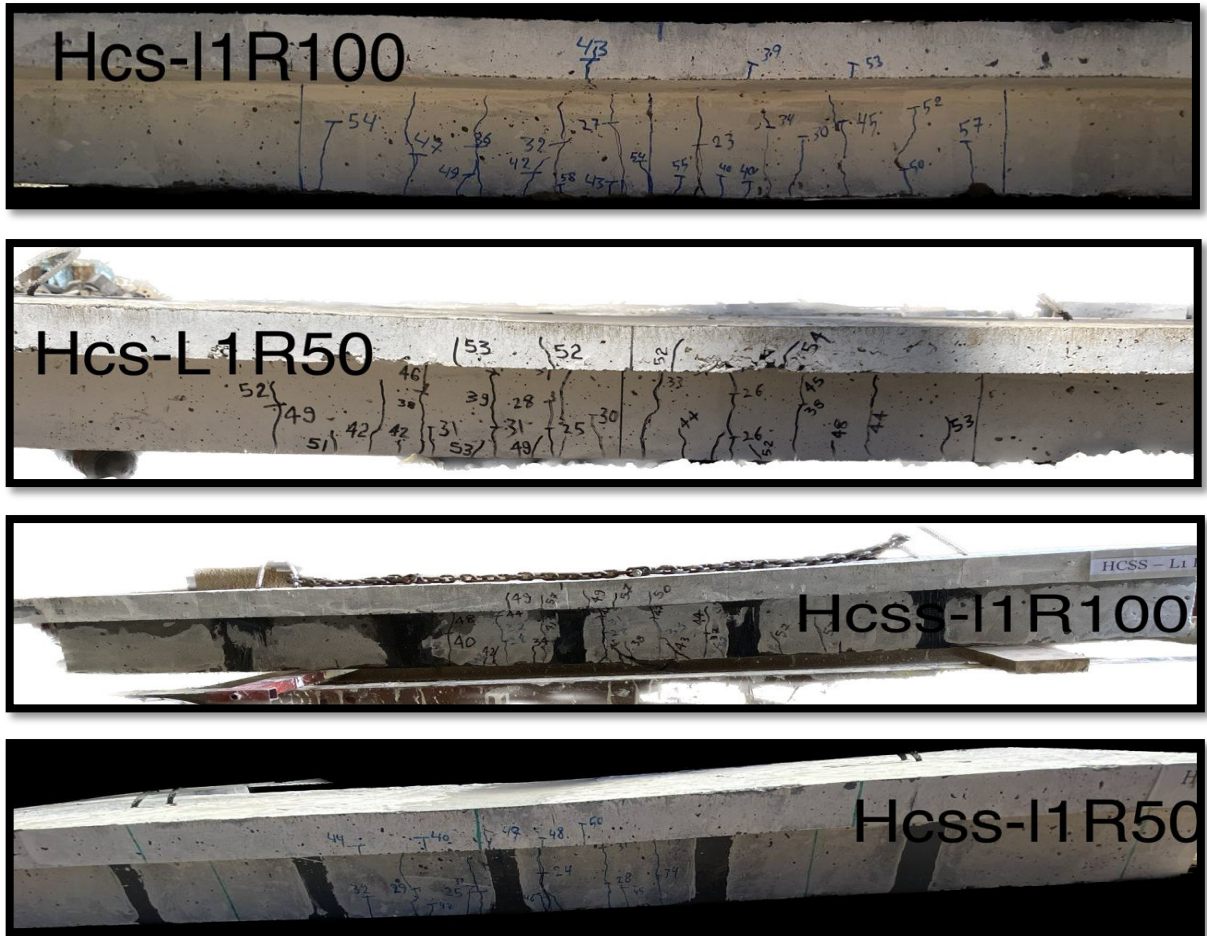


Figure 4-18 Cracks pattern for group two.

4.6.3 Group three

It is pretty similar to group two. the whole ribs warped have cracks in compression zone, they formed from tension cracks that appeared below the carbon fiber sheet and lengthen till they reach the zone that not restricted with CFRP sheet. Figure4-19 shows the crack patterns for group three.

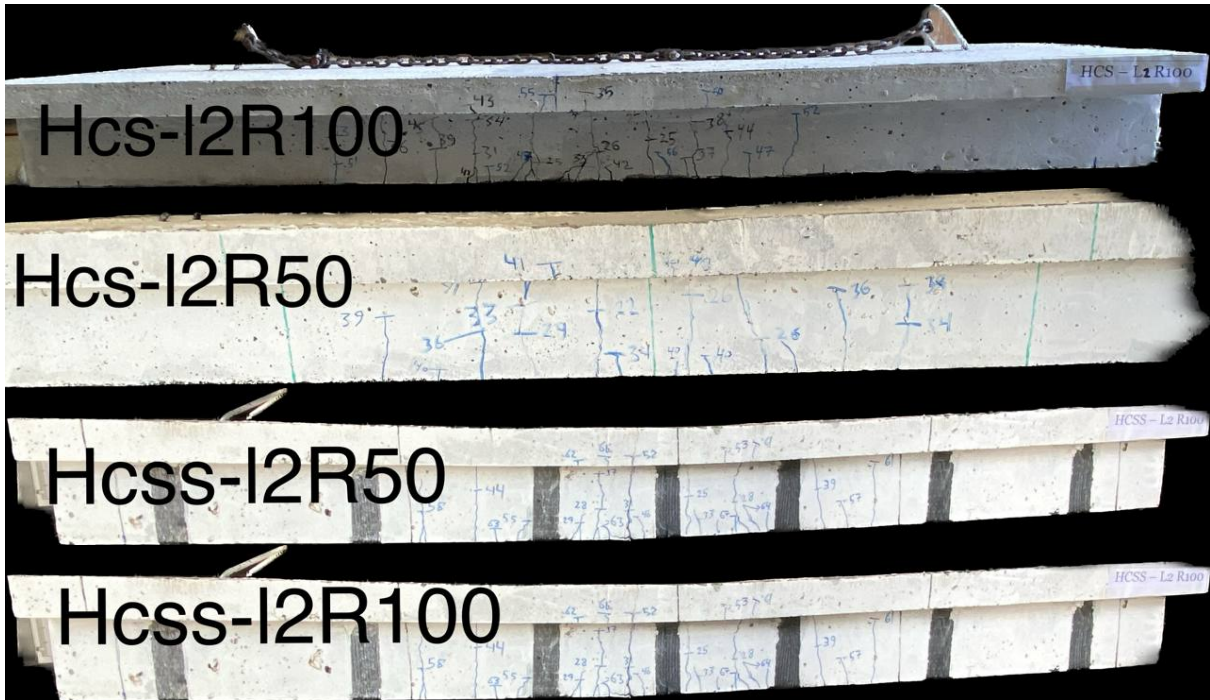


Figure 4-19 Cracks pattern of group three.

4.7 Ductility

Ductility of RC elements is defined as its ability to resist inelastic deformation without any decrease in its load-carrying capacity up to failure [38], and it is calculated by dividing the ultimate deflection by the yield deflection . The yield deflection can be obtained from the intersection of two tangential lines; the first tangential is for the elastic stage and the second for ultimate deflection [39], as shown in figure 4-20 and Table4-4

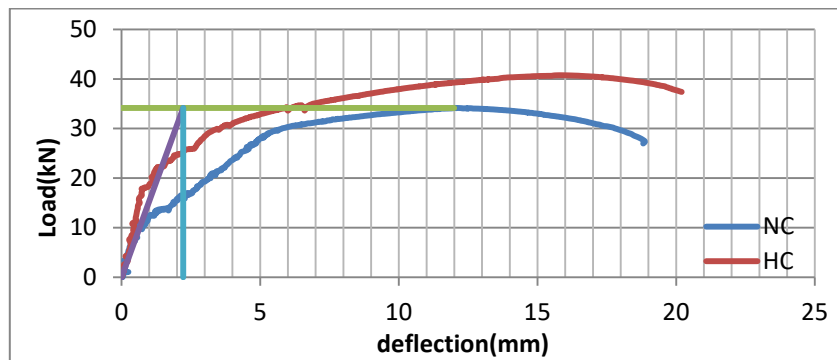


Figure 4-20 Show the method used to calculate the yielding deflection.

Table 4-4 comparing between specimens ductility.

<i>specimens name</i>	<i>Deflection at yield load (mm)</i>	<i>ductility index</i>	<i>Reduction in ductility %</i>
NC	2.22	5.39	32
HC	2	7.89	0
HCS-L1R100	2.67	5.62	29
HCS-L1R50	1.56	7.89	0.02
HCSSL1R100	1.24	8.66	-10
HCSS-L1R50	-	-	-
HCS-L1WR	3.07	4.07	48
HCS-L2R100	2.0	4.89	38
HCS-L2R50	1.56	6.51	17
HCSS-L2R100	2.44	5.98	24
HCSS-L2R50	1.51	5.61	29
HCS-L2WR	4.00	3.77	52

4.7.1 Group two

Since the carbon fiber was a brittle material, the strengthening with it led to a reduced ductility of the RC structure. The reduction percentage in ductility ranged from 34% to 46%. The whole warping ribs have the lower value and generally in this group, ductility increases with CFRP sheet width decreases for samples without strips, while samples with strips show an increase in ductility.

4.7.2 Group three

In this group, the ductility of specimens with strips was less ductile than in group two, while the opposite happened in samples with strips. Figure4-21 show the comparative of ductility for all tested specimens in group two, group three and HC.

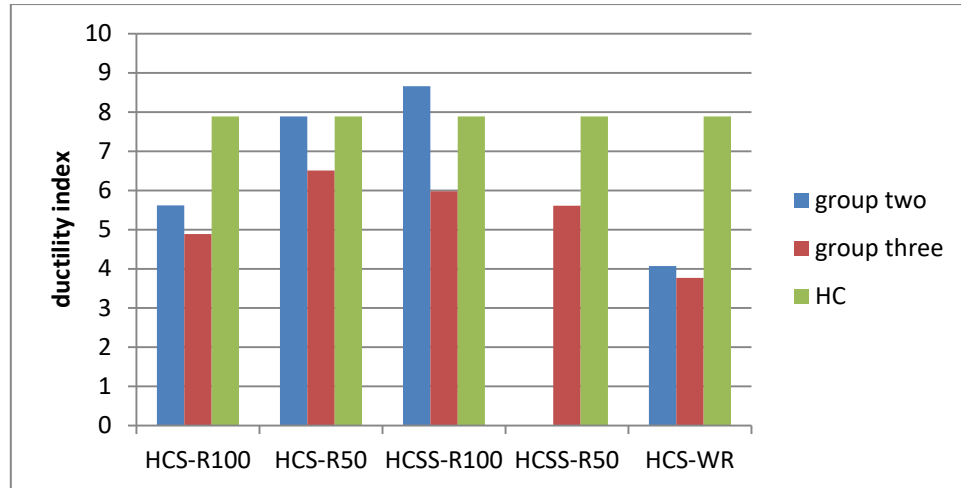


Figure 4-21 Compression between ductility of all samples.

4.7.3 Energy-Absorption.

Energy-absorption, often known as the toughness index, is defined as the area under the load-deflection curve from the initial crack deflection to the final deflection. Since it is problematic to estimate the first crack's deflection with accuracy, 1.9 mm was chosen as the fixed deflection [40]. When RC strengthen with CFRP which was a brittle material; that led to reduce toughness index. And it was found that the length of sheet was very effected on the absorbed energy [AE], except for WR samples which show large increment on AE because of it is high ultimate load ratio. Figure4-22 show ductility comparative of group two with HC and Figure4-23 show the comparative of ductility between group three and HC and the AE value were listed in Table4-5.

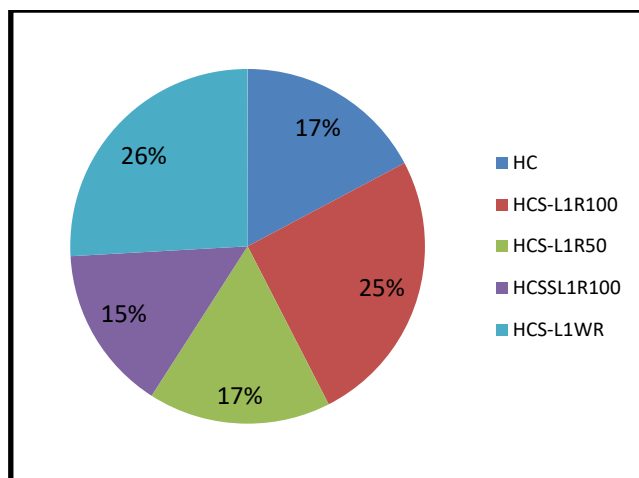


Figure 4-22 Energy absorption for group two.

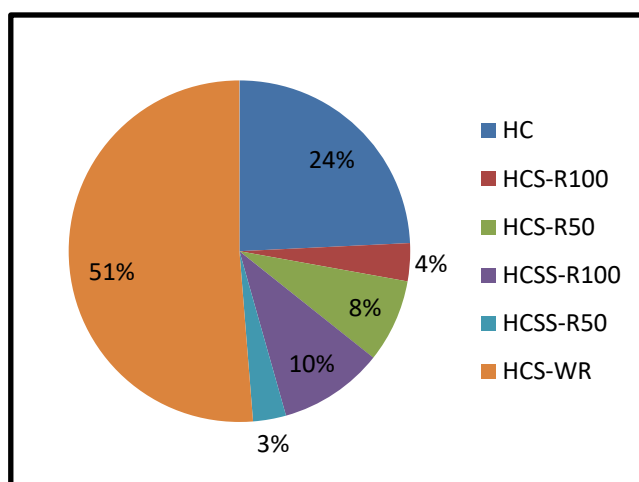


Figure 4-23 Energy-Absorption for group three.

Table 4-5 Energy-absorption values for all groups.

<i>specimens name</i>	<i>area under the curve</i>
NC	289.685
HC	499.082
HCS-L1R100	729.897
HCS-L1R50	481.125
HCSSL1R100	435.436
HCSS-L1R50	—
HCS-L1WR	749.114
HCS-L2R100	73.634
HCS-L2R50	161.929
HCSS-L2R100	203.854
HCSS-L2R50	64.502
HCS-L2WR	1054.826

4.8 Theoretical Analysis and Comparison of Moment.

All the calculation had been made in this chapter were based on both ACI440-2R [36] and previous study [41]. when the equation provides from the ACI community used, the length of CFRP sheet were neglected as it would affect the type of failure not the structural strength. So here, the experimental ultimate moment would compare twice, once with 1250mm length and with 1700mm length. Also, according to tensile flexural strength in ACI440-2R, only the sheet that was in the tension side (bottom of the ribs) was inters in calculations, both the additional strips and the carbon fiber in the side of ribs didn't account assuming it would affect the shearing strength only. But the result that achieved from the experimental program didn't have agreement with that as shown in Table4-6. The theoretical calculations made just twice; once, with 50 mm and second with 100 mm (CFRP sheets' width) and were compared with the samples with and without additional strips in addition to the whole ribs' cover in both lengths.

$T_s = A_s \epsilon_s E_s$	→	Eq.[1]
$\epsilon_s = \epsilon_c \frac{d - y}{y}$	→	Eq.[2]
$T_f = A_f E_f \epsilon_f$	→	Eq.[3]
$\epsilon_f = \epsilon_c \frac{d_f - y}{y}$	→	Eq.[4]
$M_n = T_s \left(d - \frac{\beta_1 y}{2} \right) + T_f \left(d_f - \frac{\beta_1 y}{2} \right)$	→	Eq.[5]

$$A_f = n t_f b_f$$

- C: Compressive force in the concrete.
- TS: Tension force from the steel.
- es: Strain of the steel in the section.
- Tf : Tension force from the FRP.
- ef : Strain of the FRP in the section.
- $\alpha_1; \beta_1$: Concrete compression block parameters.
- A_f : area of carbon sheet
- n: number of CFRP sheet
- t_f ; thickness of CFRP sheet
- b_f : CFRP width of CFRP sheet adjust to tension side

Table 4-6 The comparative of ultimate moment between experimental and theoretical analysis.

specimens	Theo	L1	L2	L1 With U	L2withU	L1 WR	L2 WR
HCS-R50	76.283	45.5341	37.574	45	43.0767	\	\
HCS-R100	81.392	46.0367	51.8242	53.204	63.2889	85.38173	97.9551

The neutral axis was with rib depth, so act like a rectangular section. With load raising, the neutral axis also rises and move upward the flange (slab) as shown in Figure4-24.

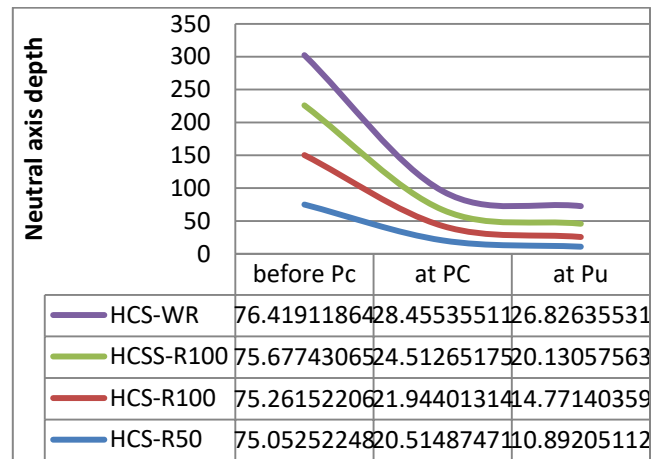


Figure 4-24 The neutral axis depth variation through the load stages.

CHAPTER FIVE
FINITE ELEMENT
ANALYSIS

Chapter Five

5 Finite Element Analysis

5.1 General

For studying the complicated non-linear structural behavior of concrete structures, in particular those with complex non-linear structural behavior, finite element analysis (FEA) is available and economical technique. ABAQUS is one of the most often used commercial finite element analysis programs for investigating structural processes and performing parametric studies[42]. The behavior of reinforced concrete (normal and high strength) and strengthening with CFRP sheet are numerically modeled using ABAQUS/CAE 2019.

5.2 Modeling of HSC One Way-Ribbed Slab strengthening with CFRP sheet.

5.2.1 Types of elements.

Many types element were used in ABAQUS to modeled the structural part. And the essential demand was choosing the right for this work. So the element types were used here was:

- ❖ C3D8R; is an eight-nodded linear 3D brick solid element with reduced integration, used to mode both the supported plates and the bearing load plate and ribbed slab[34].
- ❖ T3D2; 2-nodded linear truss elements used to model all the steel reinforcement.

- ❖ S4R5; A 4-node doubly curved thin or thick shell, reduced integration, used to model the CFRP sheet.

5.2.2 Materials' properties.

- ❖ Concrete.

The behavior of concrete was complex and nonlinear that is led to difficulty modeling concrete. The concrete damage plasticity (offered by ABAQUS) to describe quasi- brittle materials was adopted here, The Drucker- Prager flow potential yield surface proposed by Lubliner et al. (1989) [43], with the modifications proposed by Lee and Fenves (1998) [44] define the plasticity behavior of concrete by five parameters, Table 5-1 show the input data in this research based on [45].

Table 5-1 The input data of concrete plasticity parameters.

Dilation angle	37°
Eccentricity	0.1
$\epsilon_{b_0}/\epsilon_{c_0}$	1.16
kc	0.667
Viscosity parameter	0

Stress-strain curve in tension and compression required to input in ABAQUS and it was taken from BELARBI [46]. The primary characteristic of the

constitutive law of concrete in compression is the softening of peak stress in comparison. The variables that may affect the softening phenomenon were studied in a systematic manner. These variables include the tensile strain, the tensile stress, the load path and the nature of applied loads (biaxial tension-compression vs. pure shear), the percentage of steel, the spacing of steel bars, the ratio of longitudinal to transverse reinforcements, and the concrete strength. Among the variables investigated, the severity of cracking expressed in terms of E_r , the concrete strength and to a certain extent the load path found to be the main variable. The softening coefficient was also found to be inversely proportional to the graphic representation of the stress-strain relationship of the softened concrete struts is shown in Figure 5-1. The function had been used mathematically expressed as follows:

$$\sigma_d = \zeta f'_c \left[2 \left(\frac{\epsilon_d}{\zeta \epsilon_0} \right) - \left(\frac{\epsilon_d}{\zeta \epsilon_0} \right)^2 \right] \quad \epsilon_d / \zeta \epsilon_0 \leq 1$$

$$\sigma_d = \zeta f'_c \left[1 - \left(\frac{\epsilon_d / \zeta \epsilon_0 - 1}{2/\zeta - 1} \right)^2 \right] \quad 1 < \epsilon_d / \zeta \epsilon_0 \leq 1.5/\zeta$$

where ϵ_0 is the strain at the peak stress of standard concrete cylinder taken usually as 0.002 for normal strength concrete (42 MPa) and 0.0024 for high-strength concrete (100 MPa). And concrete matrix in tension was found to develop substantial tensile stresses even after extensive cracking, and the function of equation is expressed mathematically as follows (Belabor and Hsu, 1994) [47].

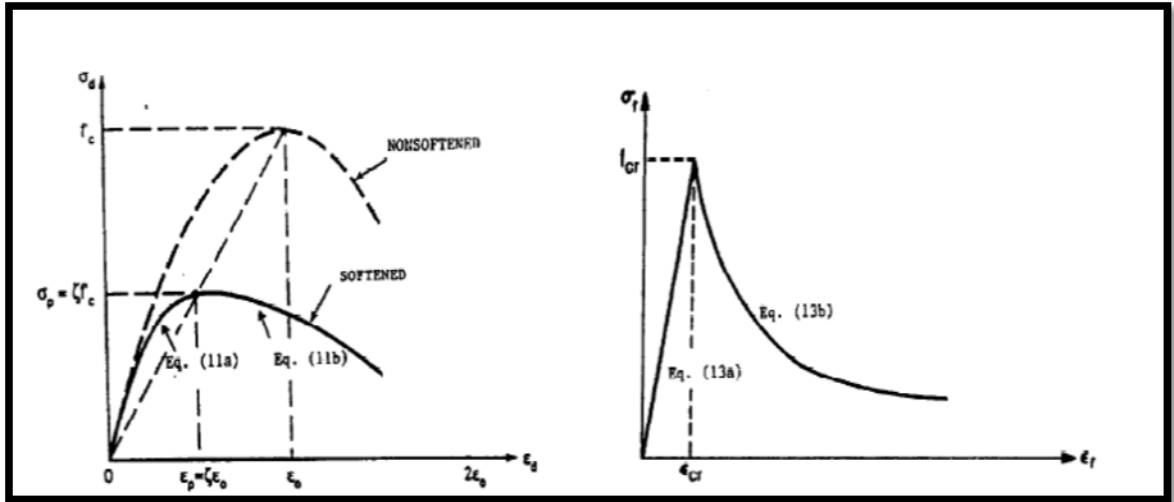


Figure 5-1 stress-strain in compression and in tension.

❖ Steel reinforcement.

Modeling of steel reinforcement done by (Hobbit et al.). The input materials required was in two ways; elastic, which define by modulus of elasticity ($E_s=200000$ MPa), Poisson’s ratio ($\nu =0.3$) and plastic which defined on table 5-2 by included yield stress and corresponding plastic strain [48].

Table 5-2 The input data for all steel’s bares and stirrups (isotropic / plastic).

plastic strain	yield stress
0	480
0.15	600

❖ CFRP sheet.

The carbon sheet was modeled as shell element and its thickness gave in the material's property. The sheet modeled as an orthotropic elastic material which have linear behavior until failure [49], the stiffness and equation were been explained in the elastic stiffness matrix below, that represent the stress –strain for CFRP.

$$\begin{bmatrix} \sigma_1 \\ \sigma_2 \\ \sigma_3 \\ \tau_{12} \\ \tau_{13} \\ \tau_{23} \end{bmatrix} = \begin{bmatrix} D_{1111} & D_{1122} & D_{1133} & 0 & 0 & 0 \\ & D_{2222} & D_{1212} & 0 & 0 & 0 \\ & & D_{3333} & 0 & 0 & 0 \\ & & & D_{1212} & 0 & 0 \\ & Sym. & & & D_{1313} & 0 \\ & & & & & D_{2323} \end{bmatrix} \begin{bmatrix} \epsilon_{11} \\ \epsilon_{22} \\ \epsilon_{33} \\ \gamma_{12} \\ \gamma_{13} \\ \gamma_{23} \end{bmatrix}$$

All the mine parameter in this matrix were defining in the equations that written below and the input data listed in table 5-3

$$\begin{aligned} D_{1111} &= E_1(1 - \nu_{23}\nu_{32})\gamma, \\ D_{2222} &= E_2(1 - \nu_{13}\nu_{31})\gamma, \\ D_{3333} &= E_3(1 - \nu_{12}\nu_{21})\gamma, \\ D_{1122} &= E_1(\nu_{21} - \nu_{31}\nu_{23})\gamma = E_2(\nu_{12} - \nu_{32}\nu_{13})\gamma, \\ D_{1133} &= E_1(\nu_{31} - \nu_{21}\nu_{32})\gamma = E_3(\nu_{13} - \nu_{12}\nu_{23})\gamma, \\ D_{2233} &= E_2(\nu_{32} - \nu_{12}\nu_{31})\gamma = E_3(\nu_{23} - \nu_{21}\nu_{13})\gamma, \\ D_{1212} &= G_{12}, \quad D_{1313} = G_{13}, \quad D_{2323} = G_{23} \\ \gamma &= \frac{1}{1 - \nu_{12}\nu_{21} - \nu_{23}\nu_{32} - \nu_{31}\nu_{13} - 2\nu_{21}\nu_{32}\nu_{13}} \end{aligned}$$

Table 5-3 The input data on the equation which were used (value took from Reddy2004[50]).

*Transverse out-plane modulus(E_3), GPa	23
*In- plane shear modulus (G_{12}), GPa	6.894
*out- of-plane shear modulus (G_{23}), GPa	4.136
*out- of-plane shear modulus(G_{13}),GPa	6.894
*Major in -plane Possion's ratio, ν_{12}	0.3
*Out-of-plane Possion's ratio, ν_{23}	0.25
*Out-of-plane Possion's ratio, ν_{13}	0.25
Characteristic tensile strength(ft), MPa	3400

5.2.3 Geometry and the Bond Condition.

Five of the experimental program' specimens were modeling here to find the perfect simulation. The samples were being modeled was HC, HCS-R50, HCS-R100, HCSS-R100 and HCS-WR. The specimens drown on three axes as followed; the longitudinal direction of the ribbed –slab was with X-axis, while the cross- section with Y and Z- axes as shown in Figure 5-2, and Figure 5-3 show the reinforcement of all specimens. The bond between concrete and all the steel reinforcements was full bond, and modeled as the steel was embedded in the concrete (the concrete was the host). While, the bond between steel plate (load & supports) and concrete was hard contact with a friction coefficient of 0.01. On the other hand, the bond between CFRP sheet

and concrete was tie constrain (concrete was the master surface and CFRP sheet was the slave). Assumed that the samples were be tested under displacement control and were simply supported, the displacement was applied 35 mm. To save time and have a privilege from symmetry, quarter of the specimen was modeled [Figure 5-4].

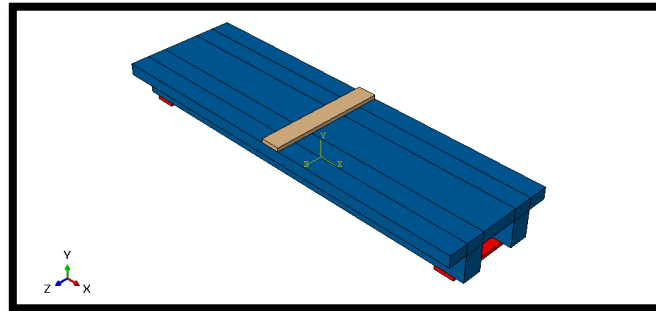


Figure 5-2 Ribbed -slab concrete modeling.

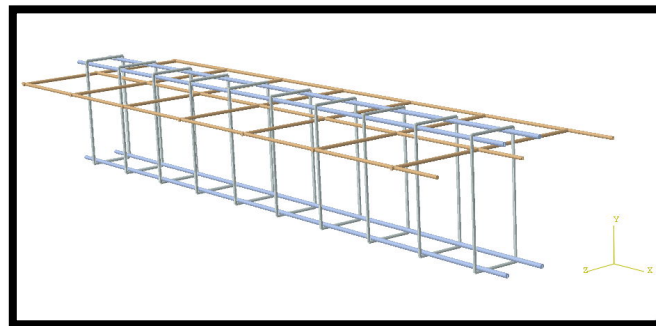


Figure 5-3 Steel reinforcement modeling.

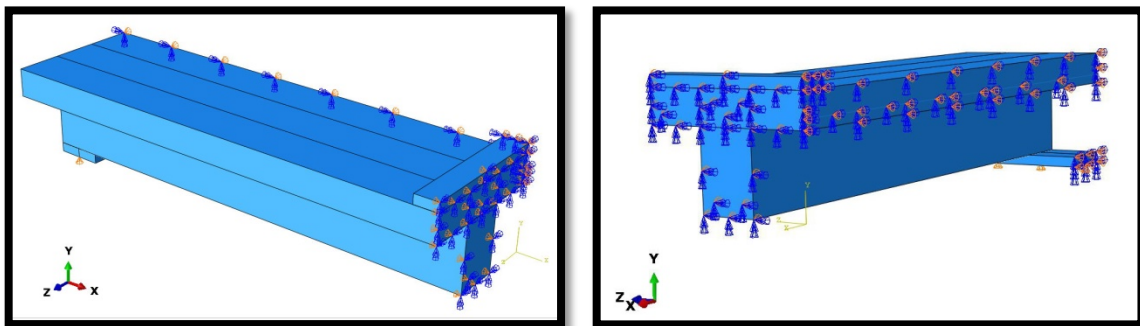


Figure 5-4 Modeling of boundary condition and symmetry.

5.3 Meshing and Converging Analysis.

The main reason of his analysis was to obtained a perfect mesh size that give a more accurate result. The analysis done on the specimen HC by using different size of mesh M30, M25, M20, M15, M10 and M8 in same applying load 37 kN and noticed the differences between M15 and M10 can be neglected.

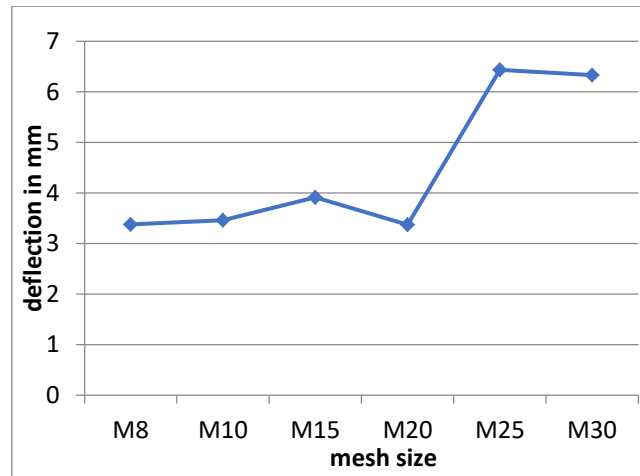


Figure 5-5 Deflection at 37 kN in different mesh size

5.4 Result and discussion.

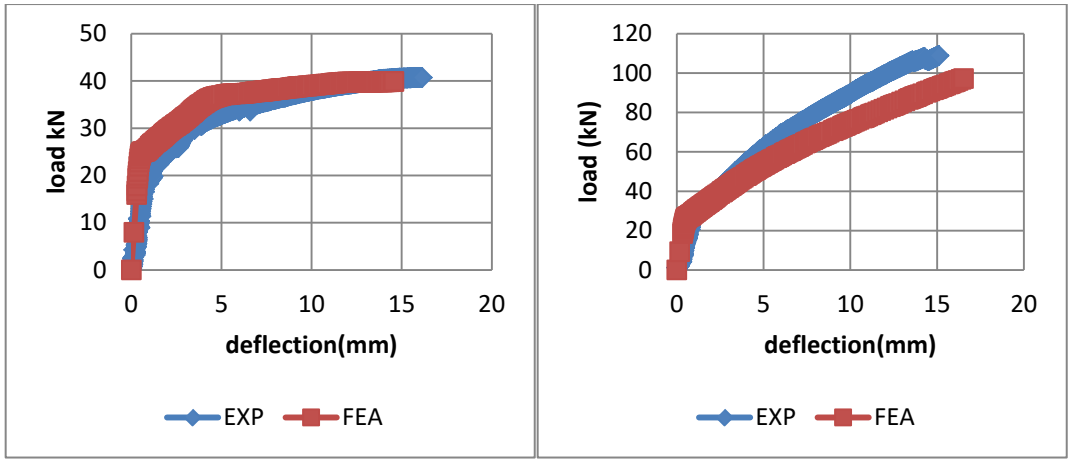
5.4.1 Load – Deflection Curve Response.

The load deflection was obtained from the experimental program were compared here with F.E modeling of the same structures. The difference in ultimate load between its, was ranged from 2 % to 19%. On the other hand, the difference in ultimate deflection between its was ranged from 1% to 7%. In this structures modeling, the F.E deflection was always more than the experimental work and that is opposite of many previous researches [51]. The deference on deflection and the ultimate load shrink as well as the CFEP sheet increased [table 5-4] show the load, deflection and the differences between

experimental and F.E analysis. Here, because the carbon sheets were bonded with the concrete by using tie bond, in other word the bond between them was assumed to be perfect so the load keep rising and since, the experimental result was existed the curve had been cut when the F.E deflection approach the experimental deflection.

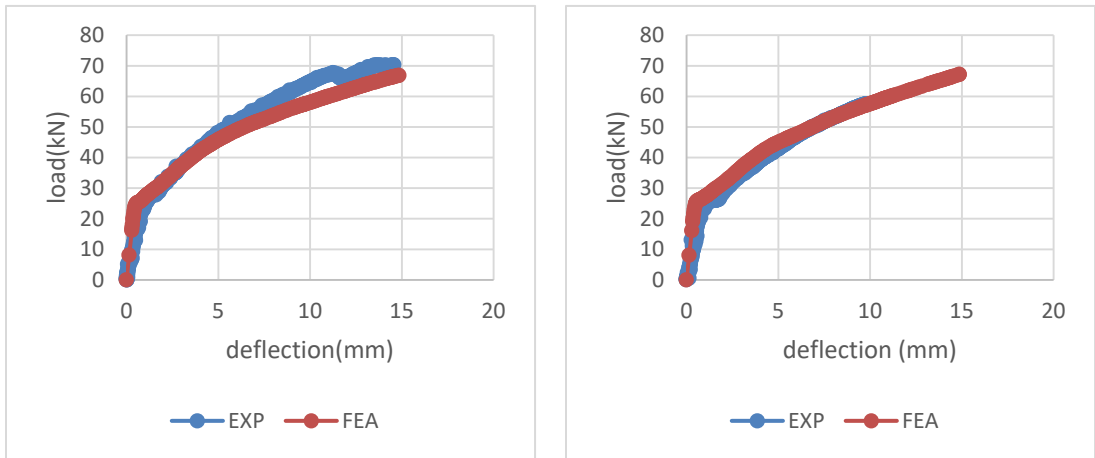
Table 5-4 the experimental and F.E analysis .

specimen's name	Experimental		finite element		deference s	
	load(k N)	def(m m)	load(k N)	def.(m m)	Load exp/F.E	Def. exp/F.E (%)
HC	40.750 96	15.775 34	39.87 87	14.563 3	2%	7%
HCS-R100	71.019 35	14.652 01	67.17 48	14.871 0	5%	-1%
HCS-R50	41.749	10.175 82	49.96 23	10.195 1	19%	0.2%
HCSS-R100	70.320 58	14.568 99	66.85 79	14.851 2	4%	-4
HCS-WR	108.83 93	15.108 67	97.21 14	16.521 9	11%	-9



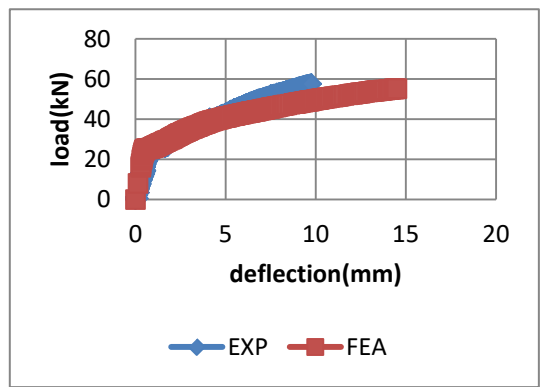
(a) Load –deflection for HC

(b) load –deflection for HCS-WR



(c) load-deflection for HCSS-R100

(d) load-deflection for HCS-R100

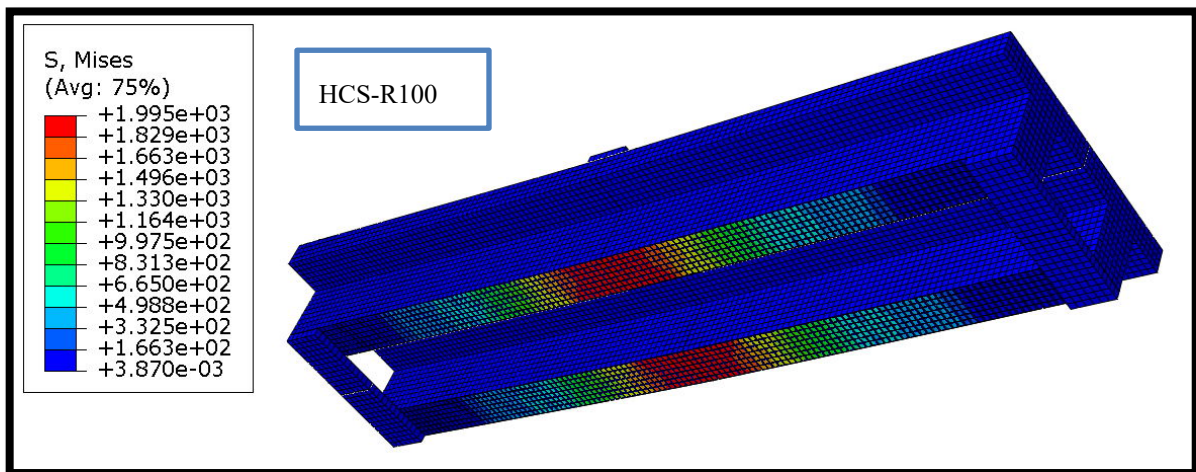
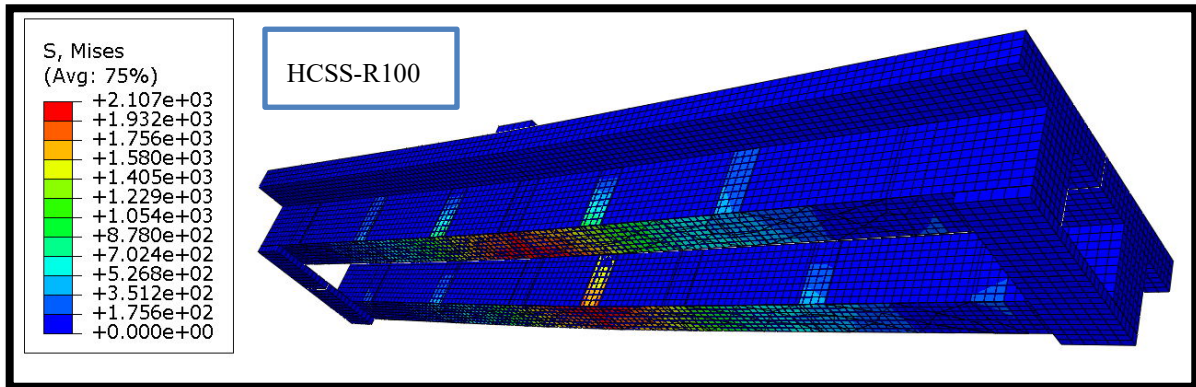


(e) load-deflection for HCS-R50

Figure 5-6 Load- deflection curve for group three.

5.5 Stress Behavior of CFRP at Ultimate load

From CFRP data sheet, the tensile stress is approximately 3500 MPa. It was appeared from the stress distribution on ABAQUS that the tensile stress reach 3494 MPa right under the load and distributed on tiny space. The tensile stress on HCS-R100 was 1995MPa and when the U-shaped stripes added the tensile stress became 2107 MPa and it was smaller than the stress of HCS-R50 in spite of increasing in ultimate load and all of that was shown in Figure 5-7 due to minimum reinforcement led to make the CFRP work with his ultimate strength beside, the 50mm sheet was not enough to strengthen the structures .



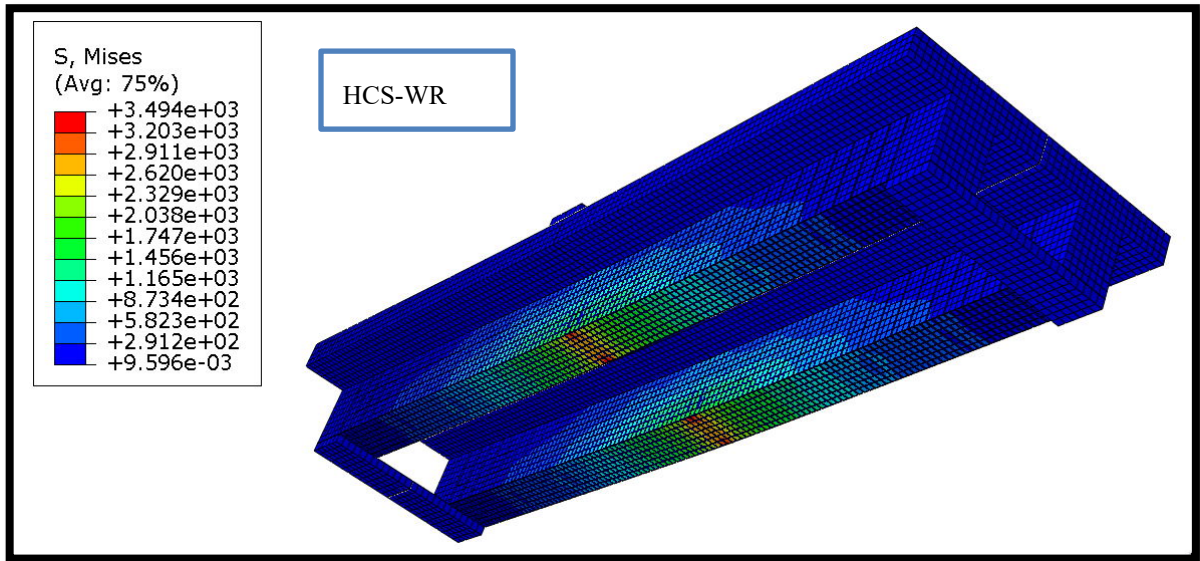
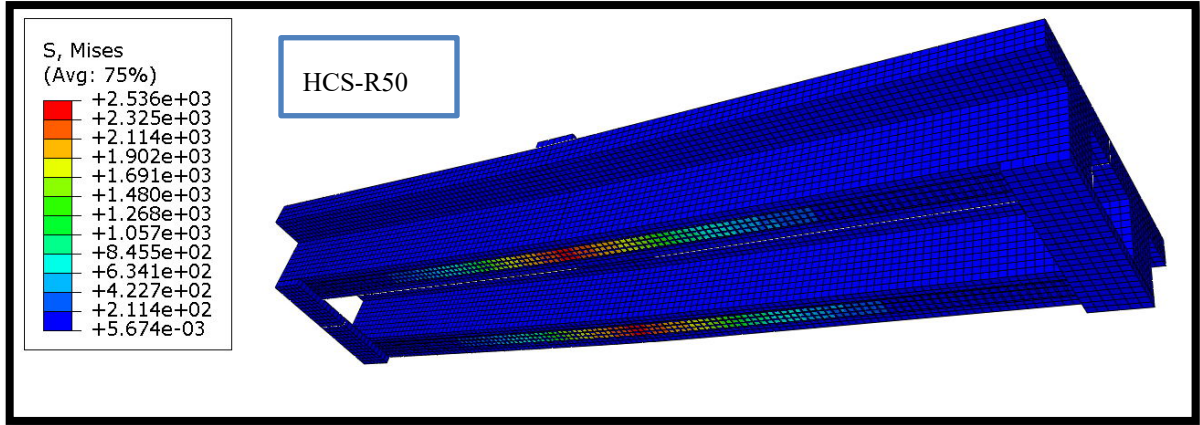


Figure 5-7 Stress distributions in modeled specimens.

5.6 Crack pattern.

The crack pattern observed in experimental were compared with that obtained from F,E and was quite similar as shown in Figure 43to Figure 47. For the reference specimen HC, the cracks were wide and concentrated in the flexural zone directly under the line load, foe other specimens; when the carbon sheet increased, the cracks were distributed on bigger space and lengthen to the flange.

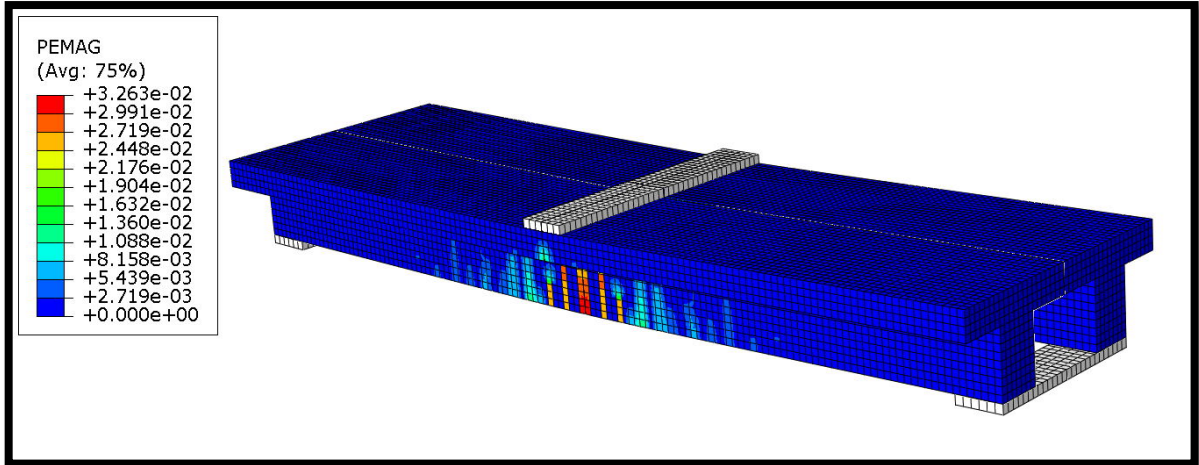


Figure 5-9 Cracks in HCS-R50



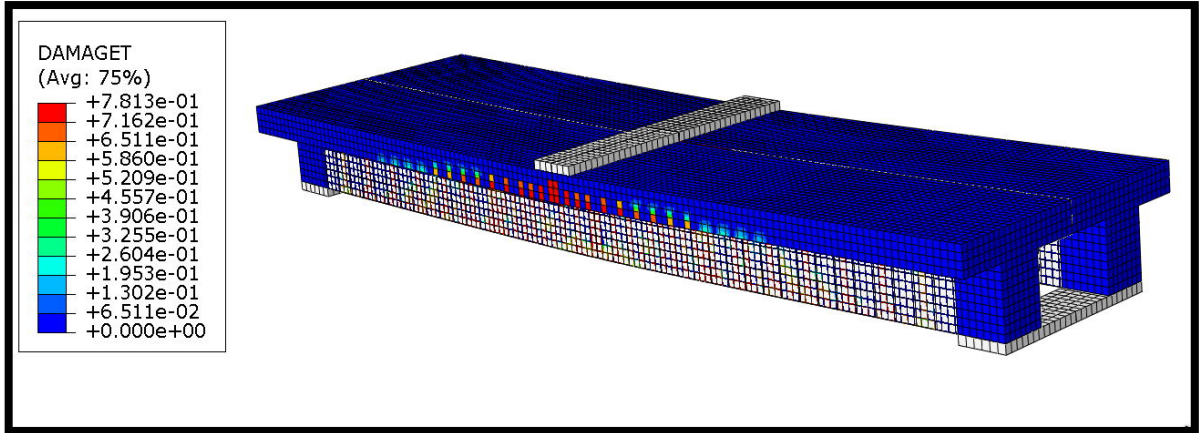


Figure 5-10 Cracks in WR.

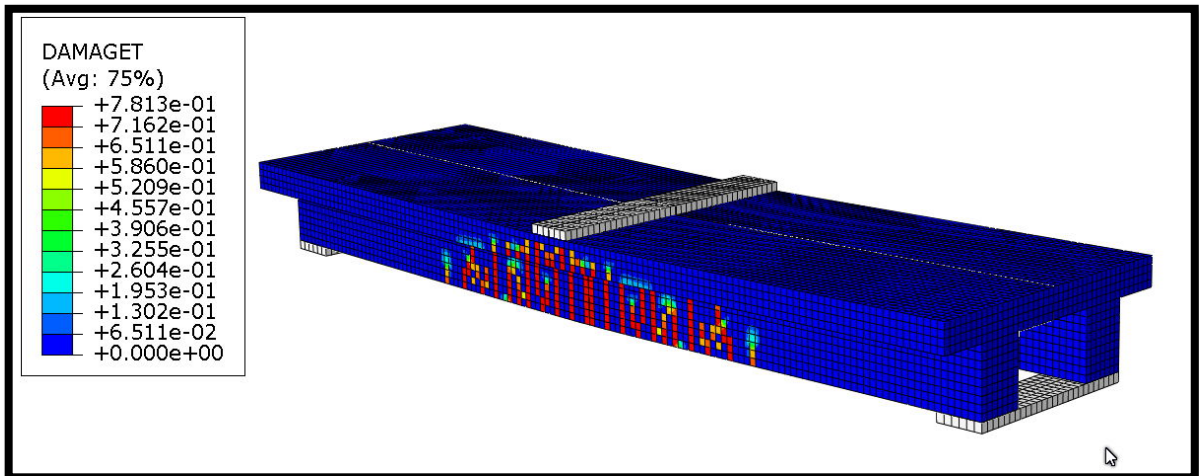


Figure 5-11 Cracks pattern in HC.

CHAPTER SIX

CONCLUSIONS AND
RECOMMENDATION

FOR

FUTURE STUDY

Chapter Six

6 Conclusions and Recommendations for Future Work.

6.1 General.

The aim of this study was improving the flexural behavior of one-way ribbed slabs by using CFRP sheets. And for that purpose, an experimental work and finite element analysis had been done as shown in the previous chapters. The main conclusions and recommendation obtained there were listed below.

6.2 Conclusions from Experimental Works.

From the experimental work, which done on three groups of samples with same geometric dimensions and steels reinforcement. The parametric study was length and width of CFRP sheets. The conclusions achieved were according to:

6.2.1 Types of Concrete.

- ❖ Casted the RS with HSC instead of NC without any strengthening, improve the flexural behavior by increasing the ultimate strength by 16% and minimize the service deflection.
- ❖ The HSC specimen was stiffer than NC specimen.
- ❖ The Absorbed Energy in HSC was higher than NC.

6.2.2 Width of CFRP Sheets.

That conclusion made to each group separately to compared samples according to CFRP sheets' width only (all the specimens had compared with HC).

6.2.2.1 Strengthening with just 1250mm length.

- ❖ Strengthening with 50% sheets width had risen the ultimate load to 35%, and to 75% with 100% sheets width
- ❖ Strengthening with 50% sheets with additional U-shape strips at 250 mm had risen the ultimate load to 23% and to 45% when 100% sheets width.
- ❖ Strengthening the whole rib was the most effect on the ultimate load by rising the ultimate load to 133% and the stiffness to 32%.

6.2.2.2 Strengthening along the clear span width.

- ❖ Strengthening with 50mm sheets width increased the ultimate strength to 3% and 41% when 100mm sheets width used.
- ❖ When using additional U-shaped strips with 50mm sheet width, the ultimate strength rises to 18% and 73% when it used with 100mm sheet width.
- ❖ Strengthening whole ribs was raised the ultimate strength to 167% and the stiffness to 26%.

Also it was found that

- ❖ The length strength didn't affect the stiffness of the structures.
- ❖ The ductility of structures decrease with any addition of CFRP.
- ❖ Energy absorption of 1250mm CF sheet length was higher than strengthening with clear span length.
- ❖ 50mm sheet wasn't enough to rise the ultimate strength.
- ❖ The ultimate deflection for all strengthening specimens less than the control specimens.
- ❖ Even though covering all the ribs had more strength and lower deflection but, it was not recommended to use due to its sudden failure.

- ❖ Adding U-shaped strips effected the strength of structures not only the failure mode.

6.3 Conclusions from FE analysis.

A FE analysis done by using ABAQUS to compared the theoretical with experimental works. Also to save time and money additional layer would be analyzed there. The analysis done on two layers only to ensure flexural failure and prevent concrete crushing. The conclusions summarized below;

- ❖ The CDM has been used to modeled the concrete and the CFRP sheets' model was an orthotropic elastic material. This model was accurate with ultimate load and the differences between the experimental works and the FE analysis was (2 to19) %, while it was less accurate in ultimate deflection with differences from (0.2 to 9) %.
- ❖ The crack pattern from FE was as similar as the one got from experimental works.

6.4 Recommendations for future study.

There were some recommendations to future investigations listed below;

- ❖ Investigate the flexural behavior of one-way ribbed slab by using different type of FRP.
- ❖ Casted the RS by light weight concrete with minimum reinforcements required and strength it with FRP.
- ❖ FE study on the RS with many parametric study such as the rib's high, width and distributions. Besides that, variable reinforcement ratio and combined types of bars like steel, glass and fiber to investigate the flexural behavior and type of failures.
- ❖ Rehabilitations the structures by using CFRP sheets and NS bars.
- ❖ study the structures ability to withstand different type of loading such as static load, impact load, dynamic load (harmonic and inharmonic).
- ❖ Study the effect of additional U-shaped stripes on deferent width and different spacing.

REFERENECES

7 References

- [1] A. F. Izzat, J. A. Farhan, and N. M. Allawi, "Behaviour and Strength of One Way Reinforced Concrete Slabs with Cavities."
- [2] Formwork solution for Paddington New Yard| Cordex <<https://cordek.com/case-study/paddington-new-yard>>
- [3] H. S. AL-Ameedee and H. M. Al-Khafaji, "Improving the flexural behavior of RC beams strengthening by near-surface mounting," *Journal of the Mechanical Behavior of Materials*, vol. 31, no. 1, pp. 701-709, 2022.
- [4] M. R. Esfahani, M. Kianoush, and A. Tajari, "Flexural behaviour of reinforced concrete beams strengthened by CFRP sheets," *Engineering structures*, vol. 29, no. 10, pp. 2428-2444, 2007.
- [5] R. Hawileh, W. Nawaz, J. Abdalla, and E. Saqan, "Effect of flexural CFRP sheets on shear resistance of reinforced concrete beams," *Composite Structures*, vol. 122, pp. 468-476, 2015.
- [6] B. Täljsten, "Strengthening concrete beams for shear with CFRP sheets," *Construction and Building Materials*, vol. 17, no. 1, pp. 15-26, 2003.
- [7] A. C. 363, *Report on High-Strength Concrete (ACI 363R-10)*. ACI, 2010
- [8] O. Gjörv, "High-strength concrete," in *Developments in the Formulation and Reinforcement of Concrete*: Elsevier, 2008, pp. 153-170.
- [9] H. M. Abdul-Wahab and M. H. Khalil, "Rigidity and strength of orthotropic reinforced concrete waffle slabs," *Journal of Structural Engineering*, vol. 126, no. 2, pp. 219-227, 2000.
- [10] J. Prasad, S. Chander, and A. Ahuja, "Optimum dimensions of waffle slab for medium size floors," 2005.
- [11] R. Shabbar, N. Noordin, E. T. Dawood, and M. Z. Sulieman, "Comparison between ribbed slab structure using lightweight foam concrete and solid slab structure using normal concrete," *J. Concr. Res. Lett*, vol. 1, pp. 19-34, 2010.

- [12] P. F. Schwetz, F. d. P. S. L. Gastal, and L. Silva F, "Numerical and experimental study of a waffle slab designed to serve as a tennis court floor," *Revista IBRACON de Estruturas e Materiais*, vol. 6, pp. 375-391, 2013.
- [13] A. J. Olawale and A. G. Ayodele, "A Comparative Study on the Flexural Behaviour of Waffle and Solid Slab Models When Subjected to Point Load," *Journal of Civil Engineering and Architecture*, vol. 8, no. 5, 2014.
- [14] H. Ahmad, M. H. M. Hashim, A. A. Bakar, and S. H. Hamzah, "Flexural behaviour and punching shear of selfcompacting concrete ribbed slab reinforced with steel fibres," in *MATEC Web of Conferences*, 2017, vol. 138: EDP Sciences, p. 02010.
- [15] P. Sacramento, M. Picanço, and D. Oliveira, "Reinforced concrete ribbed slabs with wide-beam," *Revista IBRACON de Estruturas e Materiais*, vol. 11, pp. 966-996, 2018.
- [16] T. Mohammed and H. Kadhim, "Static and Dynamic Behavior of High-strength Lightweight Reinforced Concrete One-way Ribbed Slabs," *International Journal of Engineering*, vol. 35, no. 4, pp. 732-739, 2022.
- [17] Y. J. Kim, C. Shi, and M. F. Green, "Ductility and cracking behavior of prestressed concrete beams strengthened with prestressed CFRP sheets," *Journal of composites for construction*, vol. 12, no. 3, pp. 274-283, 2008.
- [18] M. Shahawy, M. Arockiasamy, T. Beitelman, and R. Sowrirajan, "Reinforced concrete rectangular beams strengthened with CFRP laminates," *Composites Part B: Engineering*, vol. 27, no. 3-4, pp. 225-233, 1996.
- [19] V. Ramana, T. Kant, S. Morton, P. Dutta, A. Mukherjee, and Y. Desai, "Behavior of CFRPC strengthened reinforced concrete beams with varying degrees of strengthening," *Composites Part B: Engineering*, vol. 31, no. 6-7, pp. 461-470, 2000.
- [20] K. Soudki and T. Alkhrdaji, "Guide for the design and construction of externally bonded FRP systems for strengthening concrete structures (ACI 440.2 R-02)," in *Structures Congress 2005: Metropolis and Beyond*, 2005, pp. 1-8.

- [21] I. Canada, "Strengthening reinforced concrete structures with externally-bonded fibre reinforced polymers: Design manual No. 4," ed: Winnipeg Manitoba, Canada, 2001.
- [22] M. D. Abdulah, "Behavior of Reinforced Height Strengthened Concrete one Way Slabs Strengthened with CFRP Sheets," *Engineering and Technology Journal*, vol. 33, no. 3 Part (A) Engineering, 2015.
- [23] Y. Murad, "An experimental study on flexural strengthening of RC beams using CFRP sheets," *International Journal of Engineering & Technology*, vol. 7, no. 4, pp. 2075-2080, 2018.
- [24] H. Mahmoud, R. Hawileh, and J. Abdalla, "Strengthening of high strength reinforced concrete thin slabs with CFRP laminates," *Composite Structures*, vol. 275, p. 114412, 2021.
- [25] N. S. K. Al-awiady, "Structural Behavior of Pre - Loaded Reinforced Concrete Columns Under Effect of Cyclic Fire Exposure," Civil Engineerin, University of Babylon, Master of Science in Engineering, 2023.
- [26] i. A. Iraqi Specification Standards, "Portland Cement IQS No. (5)," ,*Central Agency for Standardization and Quality Control, Planning Council, Baghdad, IRAQ*, 1984.
- [27] I. S. S. No, "45—Aggregate from natural sources for concrete and building construction|| Central Organization for Standardization and Quality Control," ed: Iraq, 1984.
- [28] C. ASTM, "494. Standard Specification for Chemical Admixtures for Concrete," ed: West Conshohocken, PA: ASTM International, 1999.
- [29] B. S. Institution, *Specification for Testing Concrete: Method for Determination of the Compressive Strength of Concrete Cores*. British Standards Institution, 1983.
- [30] A. I. C. C. o. Concrete and C. Aggregates, *Standard Test Method for Splitting Tensile Strength of Cylindrical Concrete Specimens1*. ASTM international, 2017.
- [31] C. ASTM, "Standard test method for flexural strength of concrete (using simple beam with third-point loading)," in *American society for*

testing and materials, 2010, vol. 100: ASTM Michigan, United States, pp. 19428-2959.

- [32] B. Standard, "Structural use of concrete," *BS8110*, 1986.
- [33] A. Committee, "Building code requirements for structural concrete (ACI 318-08) and commentary," 2008: American Concrete Institute.
- [34] A. S. H. Abboud, "Behavior of Reinforced Concrete Thin Beams with Vertical and Horizontal Openings," Master in Engineering/civil engineering/structures, University of Babylon, the College of Engineering 2012
- [35] H. Pam, A. Kwan, and M. Islam, "Flexural strength and ductility of reinforced normal-and high-strength concrete beams," *Proceedings of the Institution of Civil Engineers-Structures and Buildings*, vol. 146, no. 4, pp. 381-389, 2001.
- [36] A. C. 440, *Guide for the Design and Construction of Externally Bonded FRP Systems for Strengthening Concrete (ACI 440-2R 2017)*.
- [37] Muthuswamy, K. R., & Thirugnanam, G. S. (2014). *Structural behaviour of hybrid fibre reinforced concrete exterior Beam-Column joint subjected to cyclic loading*. International journal of civil and structural engineering, 4(3), 262.
- [38] Park R. Evaluation of ductility of structures and structural assemblages from laboratory testing. *Bulletin of the new Zealand society for earthquake engineering* 1989;**22**(3):155-166.
- [39] Naba'a H. Abd. "NONLINEAR BEHAVIOR OF COMPOSITE TWO-WAY REINFORCED HIGH STRENGTH FIBER CONCRETE SLABS UNDER REPEATED LOAD" M,A. thesis, University of Babylon, Iraq2021

- [40] V. S. Gopalaratnam and R. Gettu, "On the characterization of flexural toughness in fiber reinforced concretes," *Cement and concrete composites*, vol. 17, no. 3, pp. 239-254, 1995.
- [41] M. Abdallah, F. Al Mahmoud, R. Boissiere, A. Khelil, and J. Mercier, "Experimental study on strengthening of RC beams with Side Near Surface Mounted technique-CFRP bars," *Composite Structures*, vol. 234, p. 111716, 2020.
- [42] A. M. Hashim, "Structural Behavior of Reinforced Concrete Horizontally Curved Box Girders with Opening Under Effect of Static and Cyclic Loads," Doctor of Philosophy in Engineering, Engineering / Structures, the University of Babylon, the College of Engineering 2022.
- [43] Lubliner, J., Oliver, J., Oller, S., and Oñate, E., "A plastic-damage model for concrete," *International Journal of Solids and Structures*, 25(3), pp. (299-326), 1989, doi: [https://doi.org/10.1016/0020-7683\(89\)90050-4](https://doi.org/10.1016/0020-7683(89)90050-4).
- [44] Lee, J. and Fenves, G.L. Plastic-damage model for cyclic loading of concrete structures. *Journal of engineering mechanics*, 124(8):892–900, 1998.
- [45] A. Bousselham and O. Chaallal, "Mechanisms of shear resistance of concrete beams strengthened in shear with externally bonded FRP," *J. Compos. Constr.*, vol. 12, no. 5, pp. 499–512, 2008.
- [46] A. Belarbi, L. Zhang, and T. T. Hsu, "Constitutive laws of reinforced concrete membrane elements," in *Sociedad Mexicana de ingenieria sismica in world conference on earthquake engineering*, 1996, pp. 1-8.
- [47] Wang, T. and Hsu, Thomas T.C. Nonlinear _finite element analysis of concrete structures using new constitutive models. *Computers & structures*, 79(32):2781 {2791, 2001.
- [48] Hibbitt, Karlsson, & Sorensen, "ABAQUS User's Manual". Pawtucket, 6th Edition, 2010.

[49] Raid A. Daud " Behavior of Reinforced Concrete Slabs Strengthened Externally with Two-Way FRP sheets Subjected to Cyclic Loads." Ph.D thesis, University of Manchester,UK,2015

[50]REDDY, J. N. 2004. *Mechanics of laminated composite plates and shells: theory and analysis*, CRC press

[51] Ahmad S.H. Abboud,"Behavior of Reinforced Concrete Thin Beams with Vertical and Horizontal Openings.",M.A thesis, University of Babylon, Iraq,2019

APPENDIX A

MasterGlenium[®] 54

A high performance concrete superplasticiser based on modified polycarboxylic ether

DESCRIPTION

MasterGlenium 54 has been developed for applications primarily in precast but also readymix concrete industries where the highest durability and performance is required.

MECHANISM OF ACTION

MasterGlenium 54 is differentiated from conventional superplasticisers, such as those based on sulphonated melamine or naphthalene formaldehyde condensate as it is based on a unique carboxylic ether polymer with long lateral chains. This greatly improves cement dispersion. At the start of the mixing process the same electrostatic dispersion occurs but the presence of the lateral chains, linked to the polymer backbone, generate a steric hindrance which stabilises the cement particles capacity to separate and disperse.

This mechanism provides flowable concrete with greatly reduced water demand and enhanced early strength.

TYPICAL APPLICATIONS

The excellent dispersion properties of **MasterGlenium 54** make it the ideal admixture for precast or ready-mix where low water cement ratios are required. This property allows the production of very high early and high ultimate strength concrete with minimal voids and therefore optimum density. Due to the strength development characteristics the elimination or reduction of steam curing in precast works may be considered as an economical option.

- High workability without segregation or bleeding
- Less vibration required
- Can be placed and compacted in congested reinforcement
- Reduced labour requirement
- Improved surface finish

MasterGlenium 54 may be used in combination with **MasterMatrix** for producing Smart Dynamic Concrete (SDC). The technology produces advanced self-compacting concrete, without the aid of vibration. For economic, ecological and ergonomic ready-mix / precast concrete production.

MasterGlenium 54 can be used to produce very high early strength floor screeds. For screed mix designs consult Master Builders Solutions Technical Services.

PACKAGING

MasterGlenium 54 is available in 208 L drums and in bulk tanks upon request.

STANDARDS

ASTM C-494 Type F & G
 BS EN 934-2

TYPICAL PROPERTIES*

Appearance	Whitish to straw coloured liquid
Relative density	1.07
pH value	4.0 - 7.0

APPLICATION GUIDELINES

MasterGlenium 54 is a ready to use admixture that is added to the concrete at the time of batching.

The maximum effect is achieved when the **MasterGlenium 54** is added after the addition of 70% of the water. **MasterGlenium 54** must not be added to the dry materials.

Thorough mixing is essential and a minimum mixing cycle, after the addition of the **MasterGlenium 54**, of 60 seconds for forced action mixers is recommended.

MasterGlenium[®] 54

The normal dosage for **MasterGlenium 54** is between 0.50 and 1.75 L/100kg of cement (cementitious material). Dosages outside this range are permissible subject to trial mixes.

MIXING

MasterGlenium 54 is suitable for mixes containing all types of Portland cement and cementitious materials as follows:

- Microsilica
- Fly ash (PFA)
- Ground granulated blast furnace slag GGBS

Note: **MasterGlenium 54** is not compatible with **MasterRheobuild** superplasticizers.

EFFECT ON HARDENED CONCRETE

- Increased early and ultimate compressive strengths
- Increased flexural strength
- Better resistance to carbonation
- Lower permeability
- Better resistance to aggressive atmospheric conditions
- Reduced shrinkage and creep
- Increased durability

STORAGE AND SHELF LIFE

MasterGlenium 54 should be stored above 5°C in closed containers or storage tanks to protect from evaporation and extreme temperatures. The shelf life is 12 months when stored as above.

The occurrence of a surface layer with **MasterGlenium 54** is normal and will have no effect on the performance of the product.

HEALTH AND SAFETY

MasterGlenium 54 contains no hazardous substances requiring labelling. For further information refer to the Material Safety Data Sheet.

QUALITY AND CARE

All products originating from Master Builders Solutions Dubai, UAE facility are manufactured under a management system independently certified to conform to the requirements of the quality, environmental and occupational health & safety standards ISO 9001 and ISO 14001.

* Properties listed are based on laboratory controlled tests.

® = Registered trademark of the MBCC Group in many countries.

MBS_CC-UAE/GI_54_09_07/v2/03_16/v3/01_23

STATEMENT OF RESPONSIBILITY

The technical information and application advice given in this Master Builders Solutions publication are based on the present state of our best scientific and practical knowledge. As the information herein is of a general nature, no assumption can be made as to a product's suitability for a particular use or application and no warranty as to its accuracy, reliability or completeness either expressed or implied is given other than those required by law. The user is responsible for checking the suitability of products for their intended use.

NOTE

Field service where provided does not constitute supervisory responsibility. Suggestions made by Master Builders Solutions either orally or in writing may be followed, modified or rejected by the owner, engineer or contractor since they, and not Master Builders Solutions, are responsible for carrying out procedures appropriate to a specific application.

Master Builders Solutions
Construction Chemicals LLC
P.O. Box 37127, Dubai, UAE
Tel: +971 4 8090800
www.master-builders-solutions.com/en-ae

Disclaimer: the TÜV mark relates to certified management system and not to the product mentioned on this datasheet



A brand of
MBCC GROUP

Theoretical calculation

Input data

$f'c = 60$	Compressive strength
$h = 200mm$	Whole depth
$h_w = 140mm$	Web's depth
$h = 60mm$	Slab's depth
$b_s = 600 mm$	Slab's Width
$b_w = 100 mm$	Rib's width
$n = 2$	Number of Ribs
$L_t = 2000mm$	Slab Length
$L = 1800mm$	Effective span.
$f_y = 420MPa$	Steel yield strength.
$\omega_c = 3503.5 \frac{kg}{m^3}$	Concrete's unit weight
$C_c = 15mm$	Concrete's cover
$d_{bar} = 6mm$	Bar's diameter
$d_s = 4mm$	Stirrup's diameter.

β calculation

since $f'c \geq 55 MPa$

Then $\beta = 0.65$

Block depth of compressive calculation

$$(d_{bar})^2 * nb * nrrib A = \frac{\pi}{4}$$

$$A_s = 113mm^2$$

$$d_t = h - C_c - d_s - \frac{d_{bar}}{2}$$

$$d_t = 178mm$$

$$a = \frac{A_s f_y}{0.85 f'_c b}$$

$$a = 1.6 \text{ mm}$$

$$e = 0.003 \left(\frac{a}{\beta * 0.003} \right)$$

$$e = 2.118 \text{ mm}$$

* calculation of loads

Self weight load on slab

$$V_{\text{total}} = b \times h_f \times L + 2 \times h_w \times b_w \times L$$

$$V_{\text{total}} = 0.128 \text{ m}^3$$

$$\gamma_c = 2243 + 6.9 \times 10^{-6} f_c^1$$

$$d_{\text{total}} = V_{\text{total}} * \gamma W_c$$

$$Wd_{\text{total}} = 287.104 \text{ kg}$$

* Modification factor (λ)

$$\text{Since } W_c > 2160 \frac{\text{kg}}{\text{m}^3}$$

$$\text{Then } \lambda = 1$$

$$P_{\text{min}} = \max \left(\frac{1.4}{f_y}, \frac{\sqrt{f'_c}}{4f_y} \right) * \frac{b_w}{b}$$

$$P_{\text{min}} = 0.00061$$

$$p = \frac{A_s}{b d} =$$

$$p = 0.0064$$

$$p_{\text{max}} = 0.85 \beta \frac{f'_c}{f_y} \left(\frac{\epsilon_{cu}}{\epsilon_{cu} + 0.004} \right)$$

$$\epsilon_{cu} = 0.003$$

$$p_{\text{max}} = 0.0338$$

S
S

$$p_{min} < p < p_{max}$$

$$p_t = 0.85\beta \times \frac{f'_c}{f_y} \left(\frac{\epsilon_{cu}}{\epsilon_{cu} + 0.005} \right)$$

$$p_t = 0.0296$$

$$p < p_t \quad \therefore \phi = 0.9$$

$$M_u = A_s f_y \left(d_t - \frac{a}{2} \right)$$

$$M_u = 8.432 \text{ kN.m}$$

$$M_u \text{ internal} = M_u \text{ external}$$

Calculation for shear

$$V_c = 0.17 \times \sqrt{f'_c} \times b_w \times d \times 1.1$$

$$V_c = 25.783 \text{ KN}$$

$$V_c \text{ for two ribs} = 51.57 \text{ KN}$$

$$V_s = \frac{A_v f_y d}{s} = 23.47$$

$$V_s \text{ for tow ribs} = 46.94$$

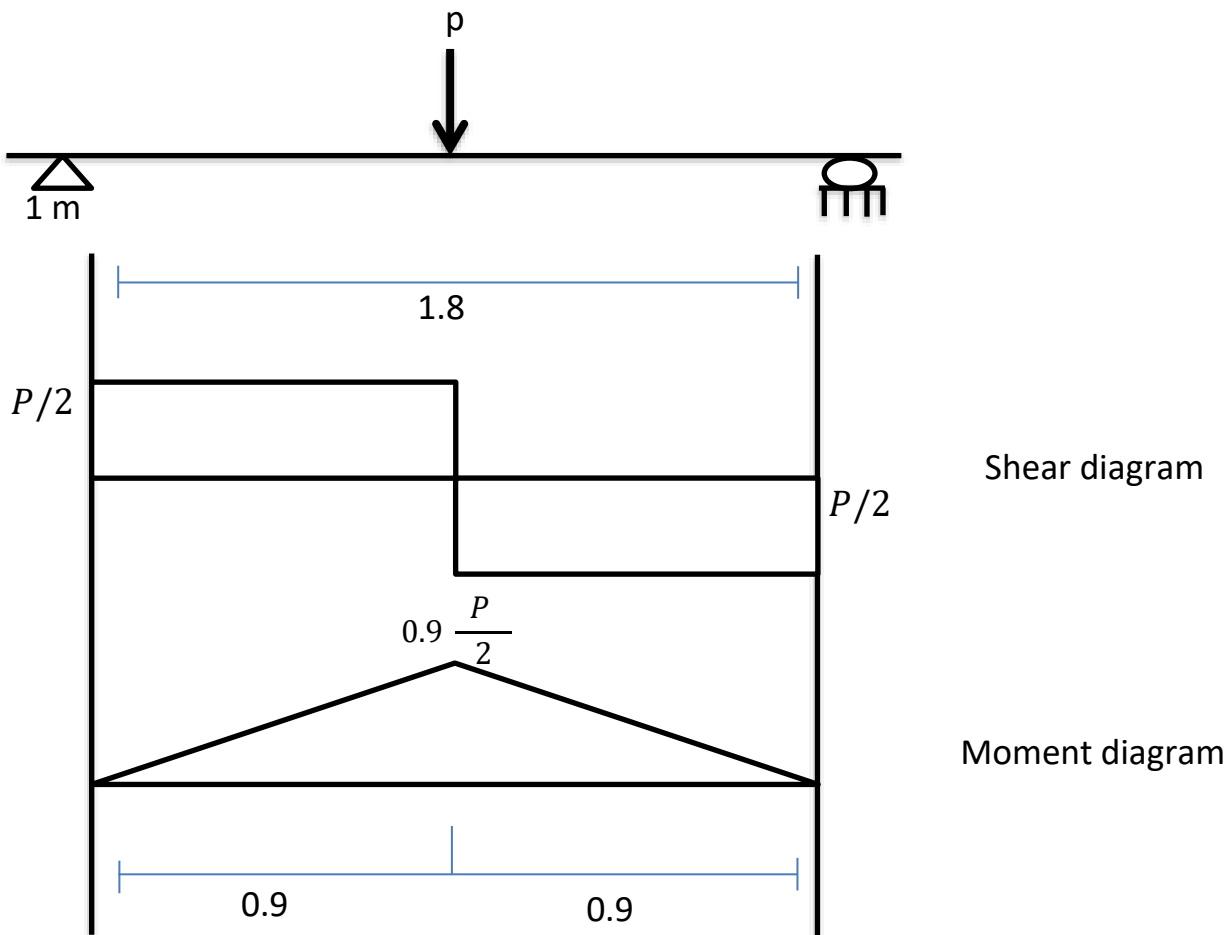
$$V_s < 4V_c \quad \therefore 0.k$$

$$V_u = V_c + V_s$$

$$V_u = 98.51 \text{ KN}$$

$$\text{Maximax shear span} = \frac{d}{2} = \frac{178}{2} = 89 \text{ mm}$$

\therefore o.K to use $\phi 4 @ 80 \text{ mm}$



$$M_u \text{ external} = M_u \text{ internal}$$

$$M_u \text{ external} = \frac{PL}{4}$$

$$\frac{PL}{4} = 8.432 \text{ KN.m}$$

$$\therefore P = 19 \text{ KN}$$

$$n \frac{P}{2} = V$$

$$\frac{P}{2} = 98.51$$

$$\therefore P = 179.02 \text{ KN}$$

Flexural load failure < Shear Load Failure

\therefore Flexural Failure

Temperature and shrinkage

$A_s = 120 \text{ mm}^2 / \text{m width}$

use mesh $\phi 5 @ 150 \text{ mm}$

4 الخلاصة

من الامور التي تم الالتفات اليها في القرن الاخير هي تقوية المنشآت أو إعادة تأهيلها لما لها من أهمية بالغة نتيجة الارتفاع السكاني او تغير وظيفة المنشأ او نتيجة الظروف البيئية القاسية التي تعرضت لها المنشآت بسبب قدمها نظرا لكون اغلب المنشآت تم بنائها خلال القرن الماضي. كذلك إعادة تأهيل المباني مهمة في المدن الي تعرضت الي هجوم ارهابي او حروب.

من أشهر المواد المستخدمة في التقوية او إعادة التأهيل هي الالياف البوليميرية بسبب مقاومتها العالية وكذلك بسبب قابليتها على مقاومة الظروف البيئية على العكس من الحديد الذي يتآكل بسبب الظروف الخارجية وكذلك لكونه غير مضر للبيئة وعميلة تطبيقه سهلة ولا تحتاج الى ايادي عاملة كثيرة.

في هذا البحث تم فحص اثنا عشر نموذج من البلاطات ذات الاعصاب احادية الاتجاه لغرض فحص مقاومة الانحناء تحت خط حمل مركز وتم تقسيم النماذج الى ثلاث مجاميع : الاولى تضم اثنان من النماذج بدون تقوية احدهما خرسانة اعتيادية والثاني تم صبه بخرسانة عالية المقاومة تصل مقاومتها الى 66 ميكا باسكال والمجموعة الثانية تتكون من خمسة نماذج تم تقويتها باستخدام الالياف الكربونية وتم تحديد عرض شرائح الكربون كأهم عنصر في الدراسة حيث تم تقوية النماذج ب 50% و 100% و تم اضافة شرائح على شكل حرف U في النموذجين التاليين اما الاخير فتم تقويته بتغليف كامل العصب , والمجموعة الثالثة تم تقوية النماذج بنفس طريقة التقوية المستخدمة في المجموعة الثانية والاختلاف الوحيد هو طول شريحة الكربون حيث كانت في المجموعة الثانية 1250 ملم بينما في المجموعة الثالثة 1700 ملم .

بعد اتمام الاختبار وتحليل النتائج تم التوصل الى ان عرض شريحة الكربون أكثر اهمية من عرض الشريحة وعلى رغم ذلك فان تقوية النماذج ب 1250ملم اعطت نتائج أفضل من ال 1700ملم. ان اقل زيادة تم الحصول عليها مع شريحة كاربون بعرض 50% من عرض العصب وكانت 3% بينما اعلى زيادة 167% مع تغليف كامل العصب وكذلك صلادة المنشأ تحسنت حيث رفعت من 5% الى 55%.

الجزء الثاني من البحث تم باستخدام برنامج ABAQUS حيث تم تحليل المنشأ واختيار موديل لتمثيل كل من الخرسانة والكاربون، حيث مثلت الخرسانة بطريقة الفشل اللدن والكاربون بطريقة الصفائح المرنة المتعامدة، وللتأكد من صحة التمثيل تم تمثيل عناصر المجموعة الثالثة وجرت مقارنتها مع ما تم الحصول عليه من الجانب العملي وكان التمثل متقارب جدا مع الجانب العملي.



وِزَارَةُ التَّعْلِيمِ العَالِي وَالبَحْثِ العِلْمِيِّ

جَامِعَةُ بَابِل - كَلِيَّةُ العِنْدَسَةِ

قِسْمُ / العِنْدَسَةِ العَدْنِيَّةِ

تحسين سلوك الانحناء للبلاطات المعصبة الخراسانية عالية المقاومة ذات الاتجاه الواحد باستخدام الياف الكاربون البوليميرية

رِسَالَةٌ تَقَدِّمَتْ بِهَا الطَالِبَةُ:

(سلوى رائد جاسم محمد)

إلى مَجْلِسِ كَلِيَّةِ العِنْدَسَةِ / جَامِعَةِ بَابِل

وهي من متطلبات نيل شهادة الماجستير في علوم الهندسة المدنية / انشاءات

بإشراف

د. (حيدر محمد جواد الخفاجي)